GAMMA RADIATION EFFECTS ON ULTRASONIC TRANSDUCERS

A Thesis

Submitted to the Graduate Faculty of the
Louisiana State University and
Agricultural and Mechanical College
in partial fulfillment of the
requirements for the degree of
Master of Science

in

The Department of Nuclear Engineering

by
Robert Wallace Smilie
B.S., Louisiana State University, 1978
May, 1983

ACKNOWLEDGEMENT

The author could not have completed this thesis, and his course of study, without the endless support shown by his family. To his wife and children, he is eternally grateful.

The author also wishes to thank Dr. F. A. Iddings for his guidance, encouragement, and time during the authors entire course of study. The author commends the entire faculty of the Louisiana State University Nuclear Science Center for their outstanding cooperation and individual dedication expressed to him over the past two and one half years.

A special thanks to Mr. L. R. Stroud, President of Stroud Sales Company, Inc., for the loan of ultrasonic testing instrumentation, without which this thesis would not have been possible. The author appreciates the cooperation of John A. Tabony and Associates Inc., in their preparation of the transducer cross section. Finally, a sincere thanks to Mrs. E. Smilie and Mr. Andre' B. Clouatre for their support and patience in the preparation of this thesis.

TABLE OF CONTENTS

LIST OF TABLES

LIST OF FIGURES

ABSTRACT

High level radioactive wastes produced in light-water reactors and from other sources must be safely and reliably stored. One method of disposal involves the use of stainless steel canisters which should be monitored remotely to assure their integrity. This may be accomplished by ultrasonic or acoustic emission monitoring.

In an effort to determine the usefulness of these test methods, several ultrasonic transducers were exposed to gamma radiation in a Cobalt-60 irradiator at several dose intervals up to a dose of 186.53 Mrads. Subsequent evaluation procedures involved multiple checks on transducer performance for sensitivity, resolution, and detectability.

It was found that the standard ultrasonic transducers in these tests failed at high radiation doses. Packaging failures prohibited evaluation beyond the 64.55 Mrad dose for all but one type of the four transducers. Radiation-induced swelling of the epoxy potting material used in the manufacture of the transducers apparently caused the wear plate to bulge and crack. Any specially designed transducer proposed for the remote monitoring of high level radioactive waste canisters should be similarly evaluated prior to use.

CHAPTER I

INTRODUCTION

Safe, reliable, and retrievable storage of high level radioactive wastes (HLW) from light-water reactors (LWR's) is of vital importance to the world's utility industry. Current technology has been developed and is being proven to store such HLW. Recently, West Germany has been storing HLW in thin-walled steel drums and stock-piling them in an underground salt dome in Asse. Other sites of waste storage have been suggested such as deep-hole burial, sub-sea burial, sea burial, salt domes, salt beds, and even outer space. Of the waste forms available, vitrified HLW in borosilicate glass seems to be the most promising.[1] France already is operating a commercial-scale vitrification plant.

The main barriers used in isolating the HLW from the environment will include the waste form, engineered barriers, and most probably, geologic barriers. The engineered barriers will consist of a continuous stainless steel (304L) canister opened only at the top and a coating of some kind (probably tar or concrete). This coating will serve to protect the canister from external corrosion, such as brine attack in a salt bed or a salt dome. It

is apparent, however, that HLW will not be stored in such an environment without a canister.

The canister itself therefore, will have to contain the vitrified HLW, provide support for this containment and finally, withstand any radiation (primarily gamma) heating. Molten glass containing the HLW is deposited in the canister through the opening at the top. There the glass solidifies and the opening is sealed by a five inch closure plug using the upset method of high current resistance welding.[2] Figure 1 is a sketch of the canister arrangement.

There is little need to monitor the upset weld while it is being made. The pressure applied to the closure plug will dictate the weld quality almost exclusively when circuit interrupters are used to control the current. However, the long term stability of the HLW canister closure-plug weld in geological formations has yet to be tested. Field conditions could certainly present longevity problems possibly not seen in a laboratory situation.

The need to monitor the HLW canister arises from the fact that leaching of the radioactive wastes from the borosilicate glass is possible if exposed to water at the elevated temperatures (200°C-400°C) and pressures (200-300 atm) likely in some of the waste storage sites.[3] If the canister's outer coating were to deteriorate, the stainless steel canister itself would be subject to corrosion and possibly erosion failure. The opening in the canister would expose the glass to a decomposing environment, possibly allowing the release of radioactive material into the geologic

Figure 1

HLW Canister Schematic

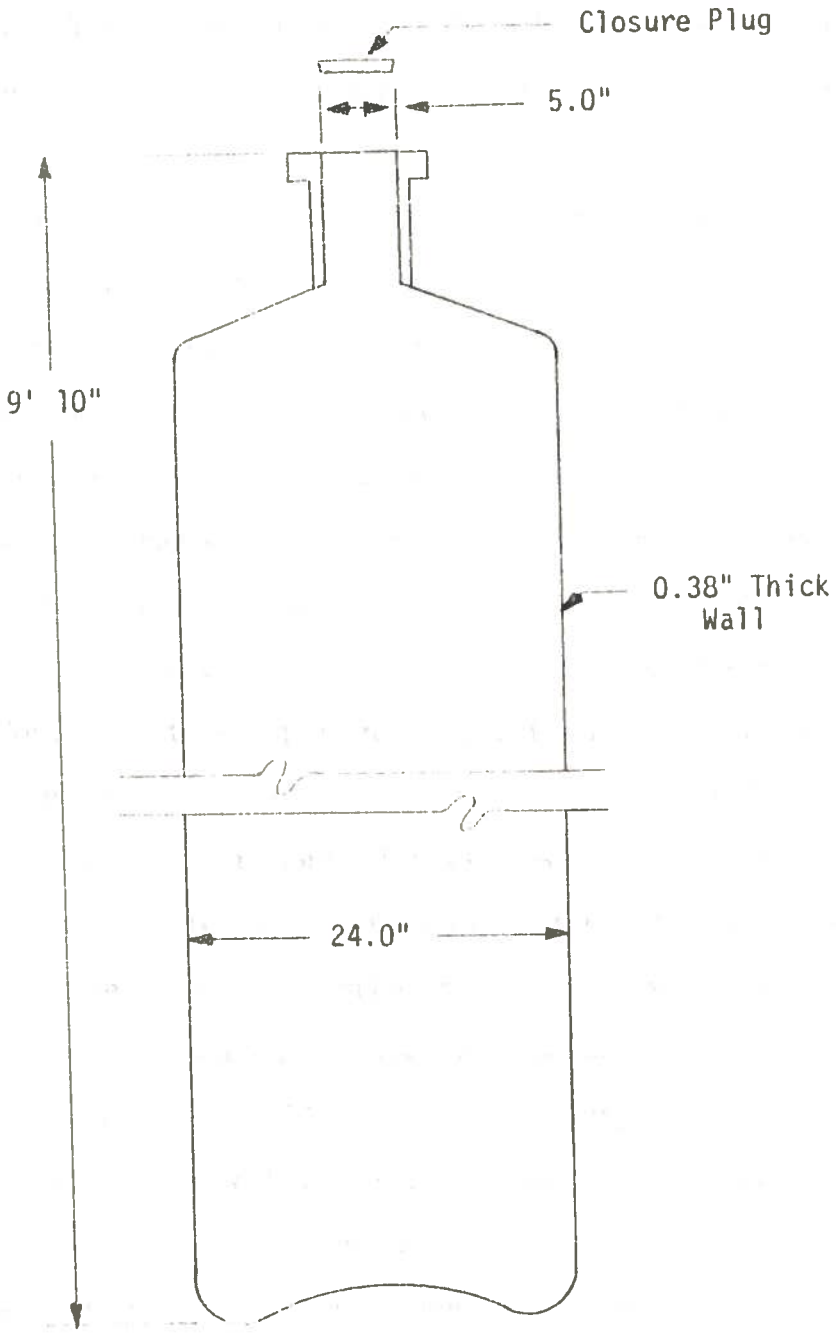

formation. The average canister will contain on the order of 3300 pounds of the glass.[4]

The feasible concept of on site monitoring of these HLW canister welded closure plugs could be realized if a determination could be made concerning the utility of the ultrasonic transducer in this application. These same ultrasonic techniques could also be used to monitor canister wall deterioration either externally or internally.

The component of the utrasonic testing system subject to the most radiation, heat, and natural environmental attack will be the transducer itself. According to Dr. Cohen, a dose rate of approximately 25 Mrad per day can be expected at a canister surface a minimum of 10 years after fuel reprocessing.[5] Through private conversations with various professionals in the nondestructive testing field who are working with LWR's, little published information seems to be available concerning ultrasonic transducers in this application.[6,7] It is important to point out that ultrasonic transducers include any transducer operating in the 20 KHz to 25 MHz range. Work has been done with low doses (10-20 Mrads) in short periods of time (0.001 sec).[8] This will not provide any basis for the objective here. Acoustic emission transducers, 20 KHz to 1.0 MHz, have been determined to have an estimated 10-year life span, if used on long wave guides when monitoring an in service LWR.[9] Private conversations with ultrasonic transducer manufacturers brought forth the fact that there is little or no interest in specially designed transducers for service in radiation fields in

the United States.[10,11] Japan, France, and Germany apparently have work underway regarding the in-service monitoring of LWR's.[12]

The objective of this thesis will be to establish the utility of ultrasonic transducers in a gamma radiation field over a period of time. This should then provide a basis for the on site monitoring of HLW canisters with ultrasonic transducers.

CHAPTER II

PRINCIPLES OF ULTRASONIC TESTING AND ACOUSTIC EMISSION

Ultrasonic testing (UT) and acoustic emission testing (AE) are both types of nondestructive testing. Nondestructive testing (NDT) is defined as the use of physical principles for detecting discontinuities in a specimen without destroying its usefulness. Nondestructive testing offers the distinct advantage of remote monitoring of the canister on site. As noted earlier, the frequency of transducer operation is one difference between UT and AE. However, the basic theory of the two methods is similar. This chapter will develop the basic theory for the two methods with primary emphasis on UT.

Ultrasonic Testing (UT)

Ultrasonic testing uses high-frequency sound waves that are introduced into the material being inspected to detect surface and subsurface discontinuities. Sound waves are mechanical waves, or particles in motion, similar to waves in water. The sound waves travel through the material and are reflected at interfaces. The reflected sound wave must then be detected and analyzed to characterize and locate the discontinuity. Sound waves have

wavelengths, frequencies, and amplitudes characteristic of the sound producing device and the sound wave medium. The relationship of wavelength, frequency, and velocity is given by the wave equation

$$V = Yf,$$

in which

V = velocity (distance/sec),

Y = wavelength (distance),

f = frequency (cycles/sec = Hz).

The two major wave propagation modes are longitudinal waves and transverse (shear) waves. The longitudinal wave has a mode of travel in which the alternating particle vibration is parallel to the direction of travel. This type of sound wave travels at the highest velocity.

For a shear wave, the alternating particle motion is perpendicular to the direction of propagation, and travels at about 50% of the velocity of the longitudinal wave in the same medium. Regardless of mode of travel, the sound wave will encounter resistance as it proceeds through a medium. This is called acoustic impedance and follows the relationship

$$Z = pV,$$

in which

Z = acoustic impedance [mass/(area-sec)],

p = density (mass/volume),

V = velocity (distance/sec).

Because the velocity of sound changes from medium to medium, so too will the acoustic impedance. The change in acoustic impedance will create an acoustic interface. The sound wave will travel through

one medium until it encounters an acoustic interface. At this point, a portion of the incident sound wave (energy) is reflected back into the first medium and a portion of it is transmitted into the second medium. The fraction of energy reflected back into the first medium is defined as [13]

$$R = (Z_1 - Z_2)/(Z_1 + Z_2),$$

in which

R = coefficient of reflection,

Z_1 = acoustic impedance in the first medium,

Z_2 = acoustic impedance in the second medium.

Optimum wave reflection is geometry dependent when a specimen is scanned for discontinuities. The ideal geometry for scanning is one in which the discontinuity is oriented perpendicular to the propagating wave front.

Sound waves can be generated and detected by piezoelectric materials. Piezoelectricity refers to the reversible phenomenon by which applied alternating voltage causes mechanical distortion and applied mechnical distortion produces an alternating voltage. Many materials with piezoelectric properties such as barium titanate, lead metaniobate, quartz, lithium sulfate, and several lead-zirconate-titanate (PZT) composites are commonly used. It was understood from a transducer manufacturer that PZT was the primary crystal material in the transducers to be irradiated in this study. A transducer is a device that will transform one form of energy to another.

The basic construction of the UT and AE transducer begins with the piezoelectric crystal.[14] As shown in Figure 2, the crystal

Figure 2

Transducer Sectional View

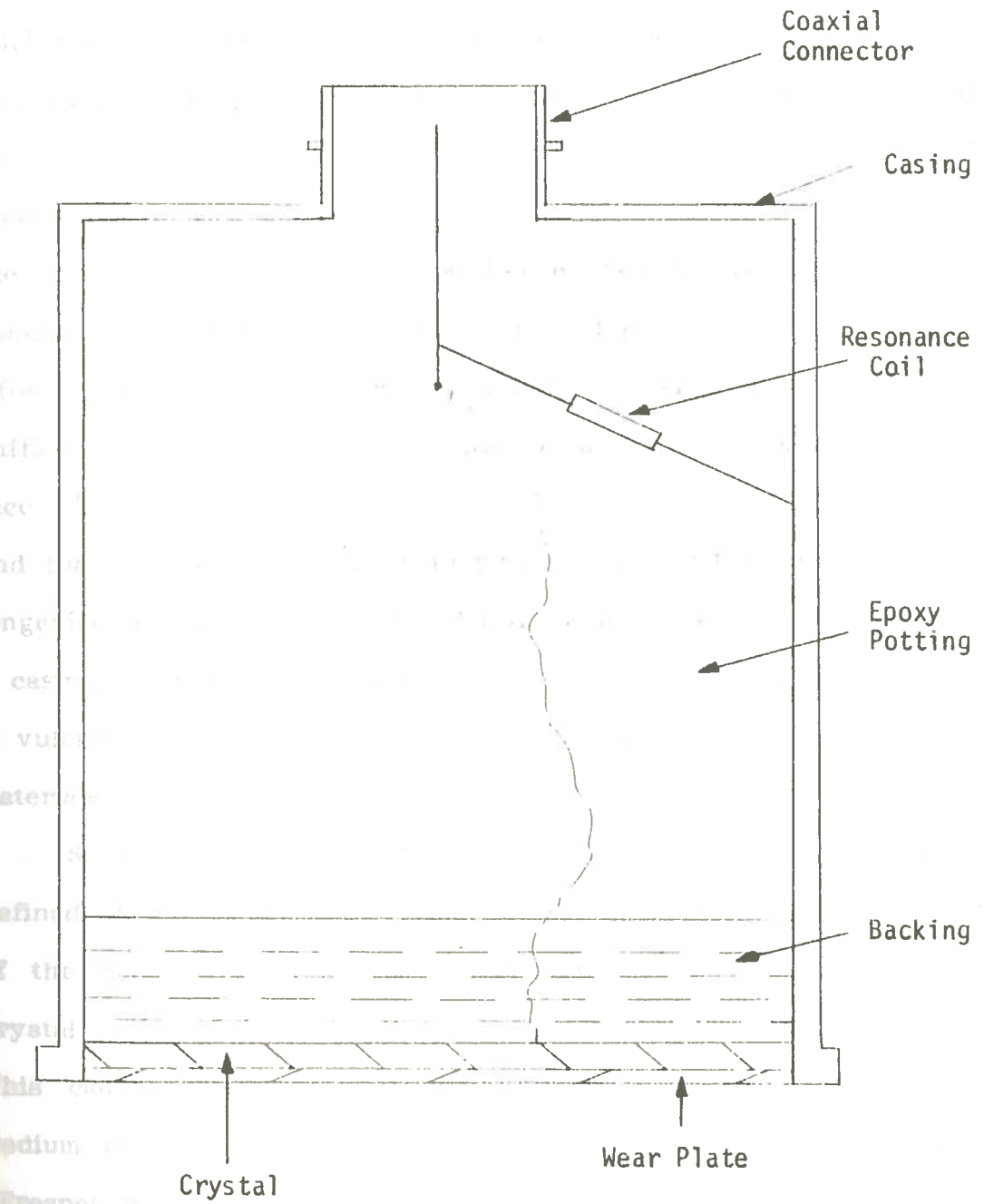

is attached to a high voltage lead on one face and to a case/instrument ground on the other. A resonance coil is usually provided in this circuit to allow maximum tuning of the transducer at a particular frequency within the limits of the crystal. The initial range of frequency for the crystal is determined primarily by its thickness. Directly behind the crystal is a backing material whose functions are to provide mounting support, control the damping of the crystal, and control the direction and number of crystal oscillations. The backing material also controls the amplitude of the sound wave. An epoxy potting is usually placed behind the backing material to isolate the high voltage lead from the case. Often, the epoxy potting can replace the backing material and will sufficiently serve both components' purposes. A wear plate, or face plate, is placed between the front electrode of the crystal and the specimen. It serves to protect the crystal and to provide longevity for the transducer. All these components are fitted into a casing usually made of stainless steel. The backing is commonly a vulcanized rubber or a molded fiber plastic. The wear plate materials used are synthetic resins, metallized epoxy, or ceramics.

Some specific characteristics of the sound beam will now be defined. They are based primarily on the frequency and the diameter of the transducer's piezoelectric crystal. The sound leaves the crystal as if it were generated by many tiny point source crystals. This causes interference effects within the region of the sound medium directly in front of the crystal known as the near field (Fresnel field). The length of these interference effects can be calculated from

$$NF = D^2 f/4V,$$

in which

NF = near field (distance),

D = diameter of crystal,

f = frequency (cycles/sec = Hz),

V = velocity (distance/sec).

At distances beyond the near field, a second field is established and is known as the far field. In this field a single sinusoidal sound wave is formed the interference effects present in the near field have ceased. The center (or peak) of the wave travels along the central axis of sound normally located through the center of the transducer crystal. Ideally, one would like to perform UT with the transducer operating outside of the near field to obtain the maximum resolution and sensitivity. The resolution of a transducer refers to its ability to separate reflected signals from discontinuities at slightly different distances. This would require the minimum ringing of the crystal; ringing is the self-damping oscillation left after wave generation. Transducer sensitivity is its ability to detect a given size discontinuity at a given distance. Sensitivity is related to the beam spread angle by

$$\sin t = (V/Df) \times 1.2,$$

in which

sin t = the enclosed angle between the central axis and the outside edge of the single wave front in the far field.

Sensitivity improves with a smaller enclosed angle. Detectability,

defined as the maximum sensitivity required to perform a particular inspection, is the transducer's ability to detect a given size discontinuity. Detectability is limited such that the critical diameter of the discontinuity is one half the maximum frequency, Y_{max}, of the sound wave. This relationship can be used with the wave equation to determine the optimum transducer frequency for a given discontinuity.

Sound wave penetration will increase with lower frequencies. Penetration is the ability of the sound wave to overcome internal medium absorption, attenuation, and scattering. The most significant of these is attenuation which is defined as

$$P = P_o e^{-aL} ,$$

in which

P_o = the acoustic pressure at the entry of the sound wave into the medium (force/unit area),

P = the acoustic pressure at the exit of the sound wave from the medium (force/area),

L = length of the medium (distance),

a = medium attenuation coefficient (dB/distance).

This is analogous to the decay equation used for radioactive materials.

An angle beam transducer is a transducer for which the incident sound beam is emitted at an angle other than normal (90°) to the test medium. In weld inspection this is normally accomplished by mounting the transducer on a lucite wedge. This allows the sound beam to undergo refraction and mode conversion. Refraction is the

change in the direction of a sound beam as it encounters an acoustic interface at an incident angle other than 90 degrees. Mode conversion is the change in the nature of the wave motion. Effectively, the incident sound beam is divided into a longitudinal wave and a shear wave within the test medium. The angle of the wave for optimum wave/discontinuity orientation can be determined from Snell's law:[15]

$$\sin i / \sin r = V_i / V_r ,$$

in which

$\sin i$ = wave angle of incidence in the incident medium,

$\sin r$ = wave angle of refraction in the test medium,

V_i = velocity of the sound wave in the incident medium,

V_r = velocity of the sound wave of interest in the test medium.

It is beneficial to reflect the longitudinal wave back into the incident medium. Interpretation is simplified with only one wave (shear) in the test medium (see Figure 3).

When the pulse-echo method is used, pulses of sound energy are injected into a test medium at regular time intervals. The energy is reflected from a discontinuity as described earlier. The discontinuity is analyzed by the amount of energy reflected and the time between the initial pulse transmission and receipt of the reflected energy. The basic pulse-echo UT instrument consists of (a) a clock, (b) an electronic signal generator, (c) a transducer (sending and receiving), (d) a reflected signal amplifier, and (e) a display device. The amplifier is calibrated in gain that is measured in units of the decibel (dB), which is a logarithmic ratio comparing two levels of power. The evaluations done in this work

Figure 3

Sound Wave Refraction

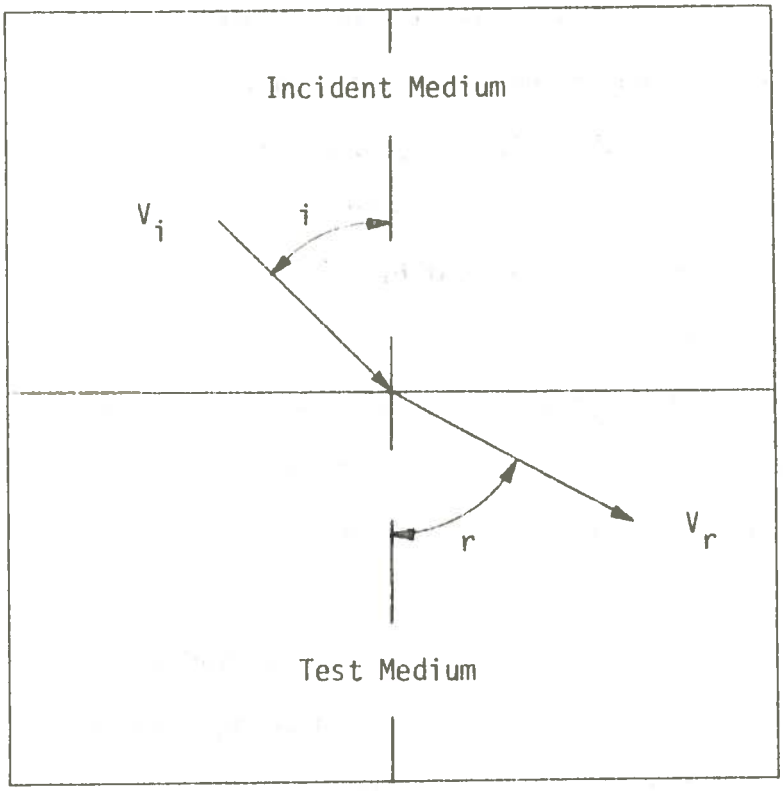

will use the A-scan oscilloscope or cathode ray tube (CRT) for the display device. It will present the reflected discontinuity signal (echo) on a two-dimensional display. The x-axis will display time of flight in units of distance, and the y-axis will display echo amplitude in terms of percent screen height. Using a calibration specimen, the screen width can be set up to a known distance. Similarly, the artificial discontinuity echo amplitude can be adjusted to a predetermined height by means of the gain.

Figure 4 is an example of the display for a single element normal-beam contact transducer on the HLW canister. In Figure 5, the display is for the angle beam transducer using a 45° lucite wedge on a butt welded steel test specimen. The transducer itself could be mounted on the HLW canister closure plug and aimed toward the outside of the neck of the canister as indicated in Figure 5. This would allow inspection of the upset weld on site. Obviously only a small portion of the weld would be inspected at one time. Several transducers may be mounted on the canister and multiplexed together to give maximum inspection coverage of the closure plug weld.

As discussed earlier, an acoustic impedance change will occur between the transducer/specimen and the transducer/wedge interface as a result of the thin barrier of air in these interfaces. This severe retardation of sound passage is eliminated by using a couplant such as glycerin, water, motor oil, or special ultrasonic gels. It is predicted that the transducers used to monitor the HLW canisters will have to be permanently mounted. This mounting must

Figure 4

Normal Beam Transducer Inspection

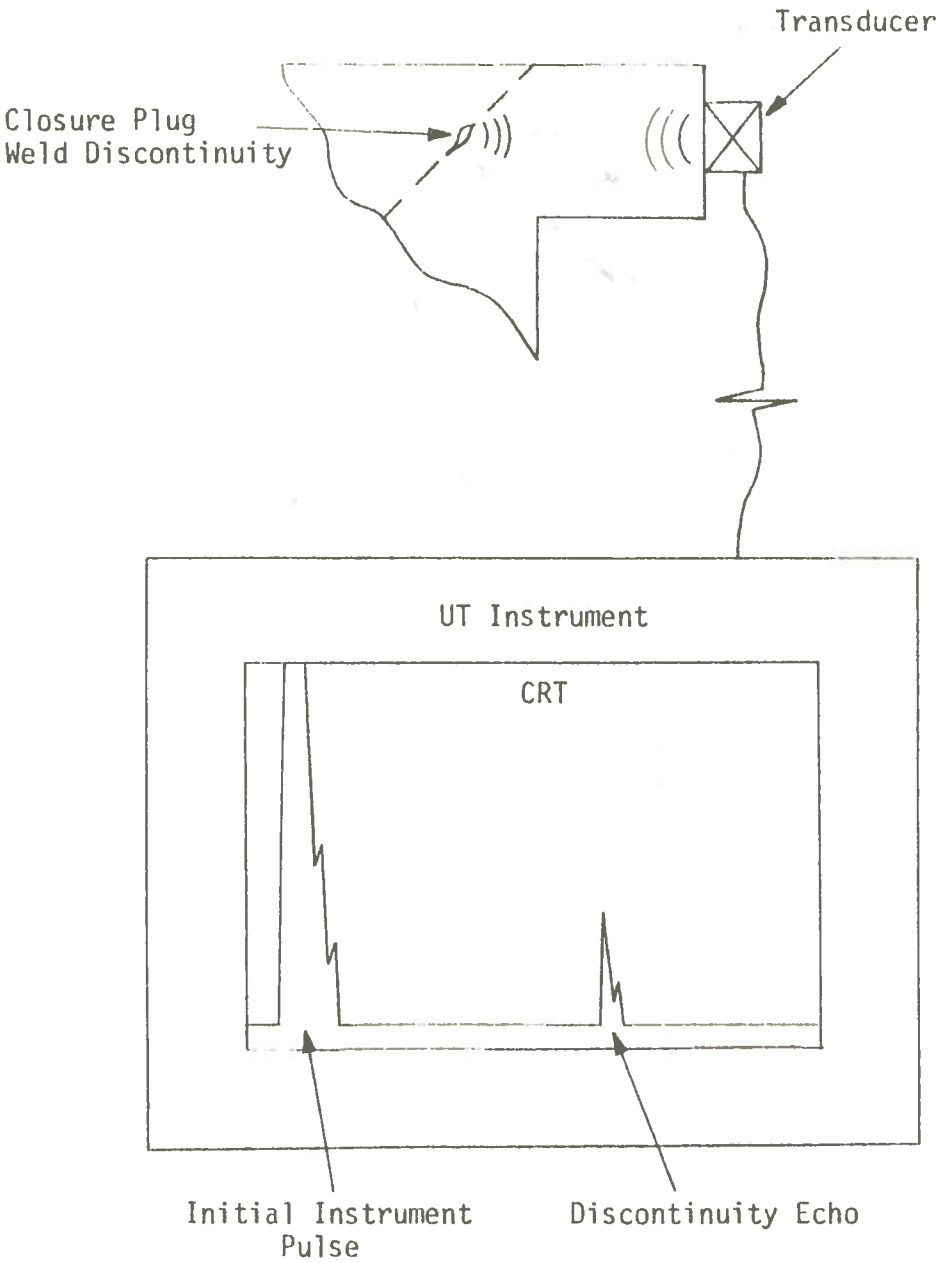

Figure 5

Angle Beam Transducer Inspection

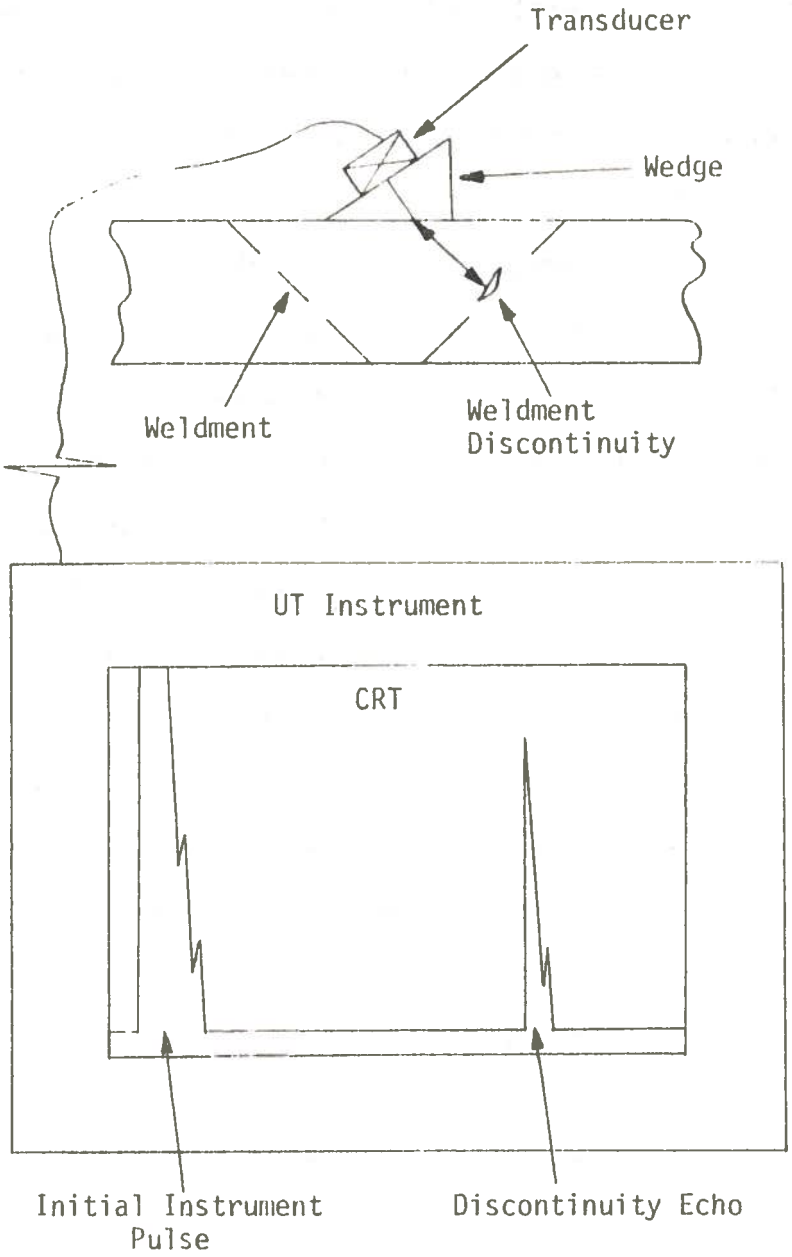

allow for good impedance matching to insure passage of the sound in and out of the canister.

Acoustic Emission (AE)[16,17]

Acoustic emission is defined as the high-frequency stress waves generated by the rapid release of strain energy that occurs within a material. The release of the strain energy comes from phenomena such as plastic deformation, phase transformations, and crack initiation and growth. Acoustic emission then requires that the test specimen be under stress. The Kaiser effect states that a specimen must surpass its previously attained stress level before the discontinuities in the specimen will have any stress-wave emissions. Many materials, including stainless steel, exhibit this effect. There are basically two types of AE: burst emissions and continuous emissions. Burst emissions are pulses of short duration and are associated with direct releases of strain energy, whereas continuous emissions are believed to be associated with dislocation movements in the grains of metals and alloys and appear as a Gaussian random noise curve. Acoustic emission is one of the most sensitive NDT methods, allows real-time inspection, and is non-directional. These advantages allow the use of AE on a wide variety of structures and materials such as fiberglass, plastic, concrete, and metal. In some cases, however, background noise prohibits the use of AE.

The AE transducer is similar in construction to the UT transducer. The sound wave is detected by the transducer, converted to an electrical signal by means of a piezoelectric

crystal, and sent on for signal processing as desired. A multitude of readout (or display) methods are available on the AE instrumentation. The selection of the AE transducer frequency is based upon the sound emitting phenomena and the amount and characterization of any prevailing background noises. Generally, AE signals are characterized by a broad band frequency spectrum.

Radiation Damage Considerations

Once the sound wave has been produced by a discontinuity in the HLW canister, an AE or UT transducer must over a period of time, be able to yield high quality information on the condition of the canister itself or on the closure plug weld. Because of similarities in construction, the UT and AE transducers should experience essentially the same radiation damage. This can be anticipated from the fact that both transducers use essentially the same individual components and should exhibit corresponding damage on a component-to-component basis. Radiation damage to UT transducers should become evident as the transducers are evaluated for changes in resolution, detectability, and sensitivity with increasing doses.

CHAPTER III

EXPERIMENTAL CONCEPTS AND PROCEDURES

A Krautkramer-Branson, Incorporated, Ultrasonic Flaw Detector Model USL-38 (Figure 6) was used for all but the last transducer evaluation.[18] The last evaluation was performed, after a cross-calibration to normalize the data, with a Branson Model 303 (Figure 7) Ultrasonic Flaw Detector.[19] Both of these instruments are equipped with the basic flaw detector circuits and a cathode ray tube (CRT), and both have 2% horizontal linearity and 1 dB vertical linearity. These instruments had been calibrated within six months prior to the beginning of the experiment. Krautkramer-Branson Aerotech transducers were selected as being representative of general-purpose industrial UT transducers. Specifications for these transduers are listed in Table 1, and photographs of the four types are included in Figure 8. The standard International Institute of Welding (IIW) Type I calibration block was used for instument calibration and transducer evaluation (see Figure 9).

Several couplants were tried in an effort to minimize sensitivity variations due to couplant viscosity. From this, Echo Laboritories Ultragel II couplant was used in the calibration and evaluation procedures. A medium-consistency grease, Dow Corning

Figure 6

Model USL-38

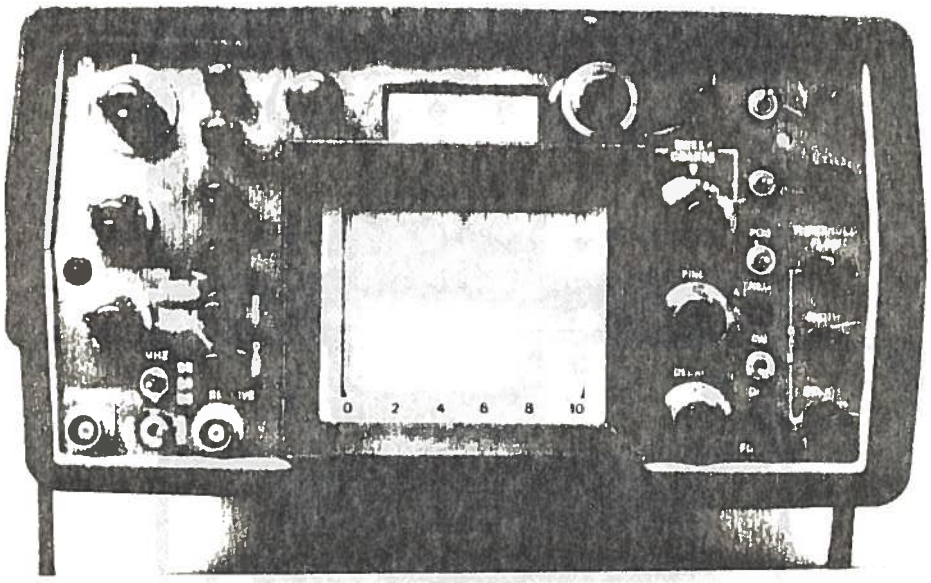

Figure 7

Branson Model 303

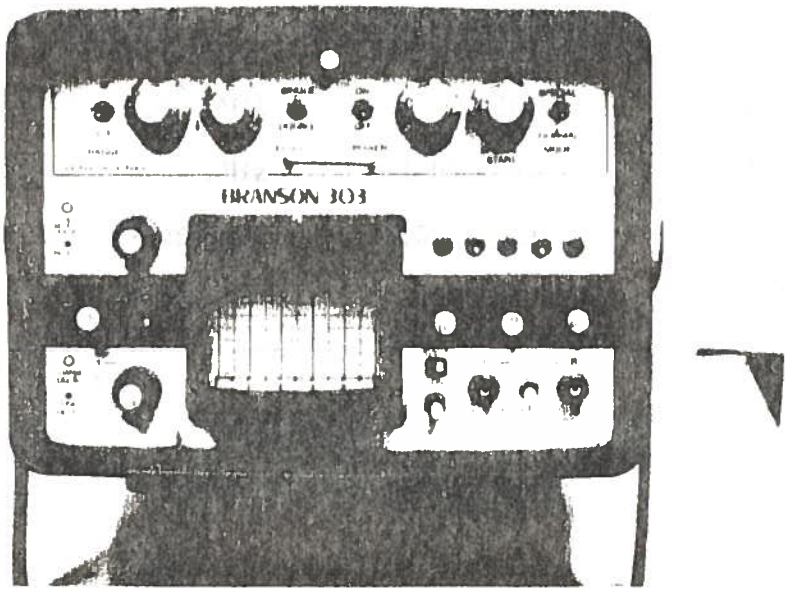

TABLE 1

List Of The Evaluated Transducers

Type	Style	Frequency	Element Size	Serial Number
L	CR	2.25 MHz	1.0" dia.	L03412
C	CR	5.00 MHz	1.0" dia.	C04401
B	SWS	2.25 MHz	0.5" x 1.0"	B16821
E	MSWS	5.00 MHz	0.5" dia.	E18902

Figure 8

The Evaluated Transducers

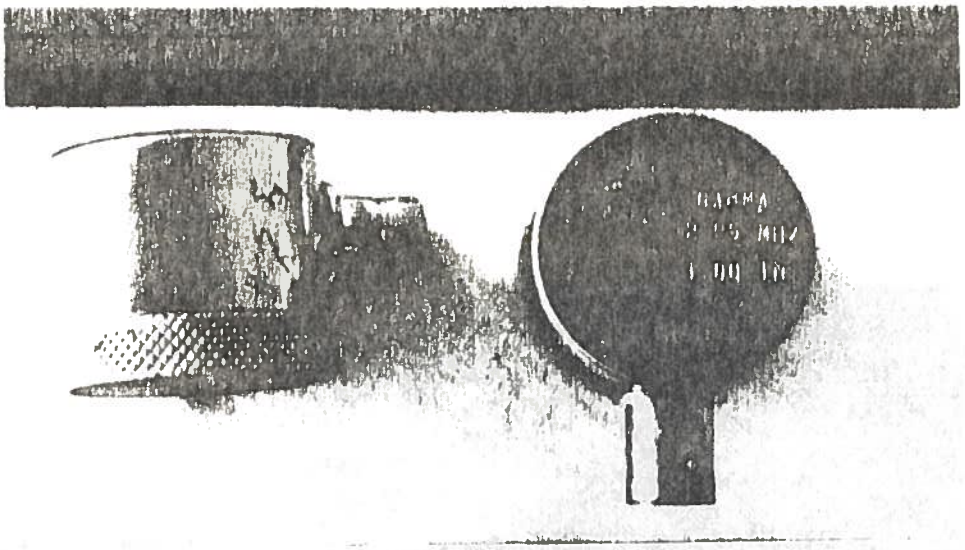

Type C

Type L

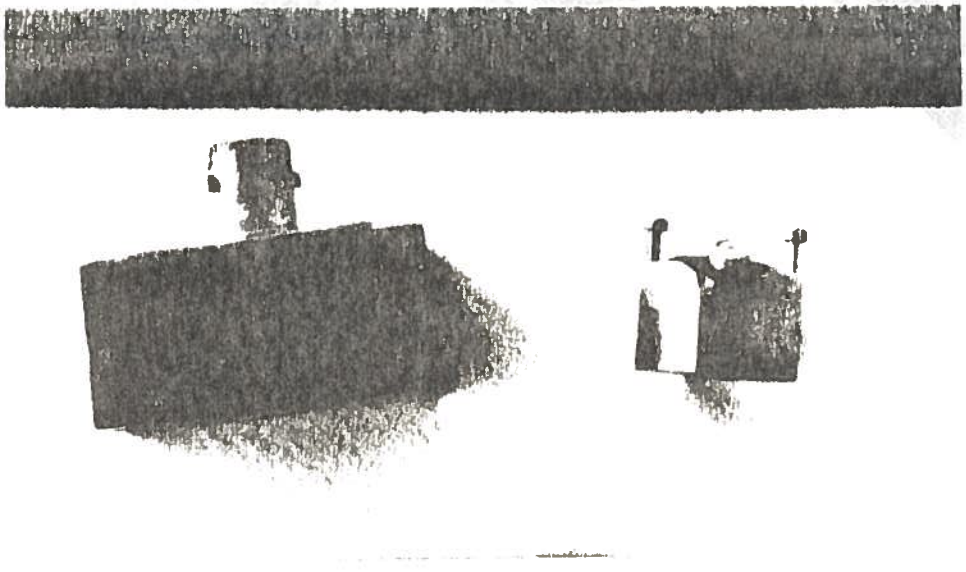

Type B

Type E

Figure 9

IIW Type I Calibration Block

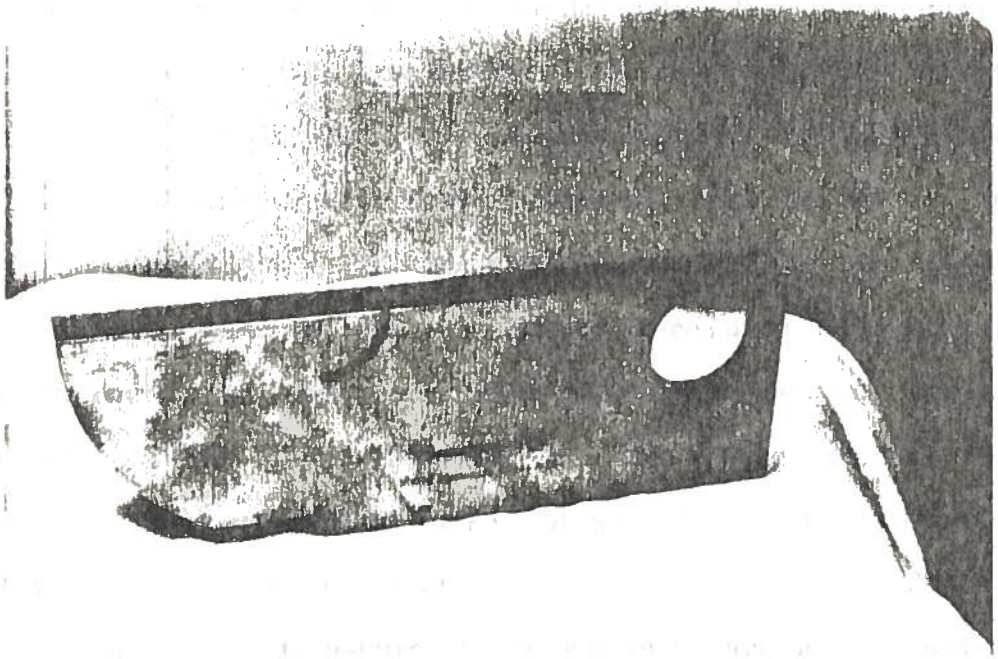

Molycote DC 44, was used between the transducer and the lucite wedge.

It was found that pressure on the transducer varied the amplitude of the IIW block artificial defect signal from 1 dB to 10 dB. The solution to most of the "pressure" effects was to use a constant force generated quite nicely by a steel block. The block was placed on top of the normal beam transducer. This was not satisfactory in the case of the angle beam transducers because of their small physical size; hence, an operator "feel" had to be developed for a consistent pressure on the angle beam transducers.

On almost any UT flaw detector, the most sensitive vertical region of the screen is 60% to 100% of screen height. It was decided that this would be the region of interest and that the 90% screen height line would be established as the desired artificial-defect reference line. Both of the instruments were used with minimum circuit tuning. The reject, or noise suppression control, was set in the off position. The damping, or pulse voltage control, was set in the position of maximum pulse voltage. The settings described above were maintained in an attempt to keep the effects of these controls minimal, and to assure overall minimum variation throughout the evaluation of the transducers.

Calibration Procedures

For the normal beam contact transducer calibration, the 1.0" thickness of the IIW block was used to set up a 2.0" screen width. The transducer was then placed directly above the 0.062" diameter hole (see Figure 10A). The gain needed to set this artificial

Figure 10

Transducer/Test Block Arrangements

A.

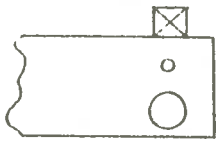

B.

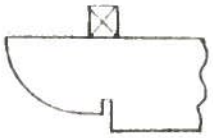

C.

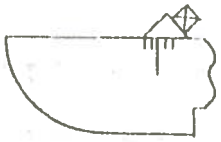

D.

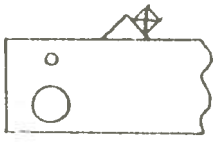

E.

defect reflection at 90% amplitude was recorded. The horizontal location and the percent of screen width of the pulse was also recorded.

The 1.0" thickness of the IIW block was again used to calibrate the screen to 5.0" full width. With the same transducer positioning, the gain was increased and recorded so that the second reflection from the plexiglass plug was placed at the desired reference line. As before, the horizontal location and the pulse width was recorded. With the transducer positioned as in Figure 10B, the gain was set so that the 3.6" reflection leading edge just touched the baseline. The gain for the desired reference line and the 3.6" pulse width were recorded.

For angle beam calibration, the sound exit point and the wedge angle were checked as in standard weld inspection procedure (see Figure 10C). If the exit point was to the left of the index mark on the IIW block, then it was classified as "under" standard. If the exit point was to the right, it was "over" standard. Using the 4.0" radius and the roll-over calibration technique, the screen was set up for 5.0" full width. This was done in the position shown in Figure 10C. The transducer was then placed in the position shown in Figure 10D. Once the 0.062" hole reflection was maximized in signal amplitude, the gain was adjusted so that the reflection just touched the 90% amplitude line. The gain, horizontal location and pulse width were recorded. In an attempt to simulate a crack in a specimen, a small block of aluminum that had been cut, machined and then bolted tightly back together was used for this phase of the evaluation (see Figure 10E). Again, the amplitude of the reflection from the crack was maximized. Several "peaks" were found within the

specimen. A decision was made to use only one position on the aluminum block. This position was scribed on the block so that it was readily located, and a specific reflected signal from the crack was then selected. It was found to occur at the 20% screen width location. The pulse amplitude was set at the 90% reference line and the gain and pulse width were recorded. This calibration method will provide the data necessary to determine the effects of the radiation on the transducer parameters given earlier.

Data Acquisition

The radiation effects on resolution will become apparent as the pulse width broadens. Sensitivity losses will be seen as a needed increase in gain to acquire the 90% reflected signal amplitude. The initial parameter to document a loss of detectability will ultimately be the loss of a detectable reflection from the 0.062" diameter hole.

A transducer data log was devised for the data acquisition. The logs include the calibration and evaluation data, are supplemented with comments necessary to explain the procedure, and are found in Chapter IV. Log no. 4 (Table 2) is inserted here as an example of the procedure followed. It is an average of three separate pre-irradiation evaluations performed on each of the four transducers. Table 3 is a list of the tolerances of each of the parameters in the logs; tolerances C through G are attainable from the operator's interpretation of the data presented on the cathode ray tube (CRT).

The transducers were irradiated at the Louisiana State University Nuclear Science Center Co-60 facility (see Figure 11).

TABLE 2

Transducer Data Log Number 4

DATE: 6/25/82 IRRADIATED FROM: Pre-Irrad. Analy. TO: --

TRANSDUCERS EXPOSED: 0 Minutes TOTAL EXPOSURE TO DATE: 0.0 Mrads

Trans. type	Wedge exit point	Trans. angle Loc./ angle	Full screen (in.)	0.062" Hole Loc./ %width	0.062" Hole dB/ %amp.	Second Plex. Reflection Loc./ %width	Second Plex. Reflection dB/ %amp.	3.6" Reflection Maximum dB at baseline dB / %width	Crack Reflection Loc./ %width	Crack Reflection dB/ %amp.
L			2.0	30/11.	48/94					
			5.0			79/4.	58/92	33/4.		
C			2.0	29/8.	44/91					
			5.0			79/4.	66/93	38/4.		
B	As marked	60/45°	5.0	18/3.	67/96				41/2.	48/93
E	1 div. under std.	60/45°	5.0	16/3.	69/91				41/2.	37/92

TABLE 3

Data Log Parameter Tolerances

Parameter	Tolerance
A. Wedge Exit Point	± 0.5 divisions
B. Transducer Wedge Angle	± 1.0°
C. Full Screen Width	± 1.%
D. Horizontal Location	± 1.%
E. Percent Screen Width	± 1.%
F. Gain	± 1. dB
G. Percent Amplitude	± 1.%
H. Exposure Time	± 15 min
I. Total Exposure	± 0.01 Mrads

Figure 11

Irradiation Facility

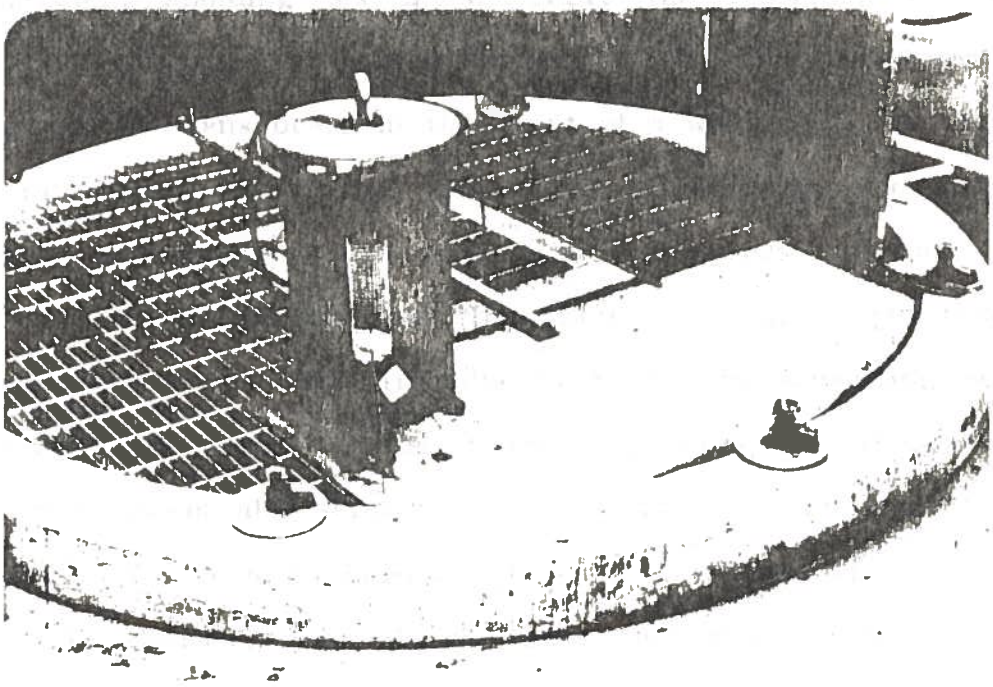

The vessel used to lower, hold and raise the transducers from the pit is approximately 18 inches high by 10.5 inches in inside diameter. Several lead bricks were placed in the vessel to aid in submerging it into the "crown" source. The "crown" source consists of twelve separate plaques, 13 inches long by two inches wide by 1/8"-1/4" thick. The approximate plaque strength during the time of the experiment was near 500 Ci each for a total combined source strength of near 6000 Ci.

A transducer basket measuring eight inches high by two inches in diameter, standing six inches above the vessel bottom was fabricated from one-quarter inch hardware cloth. The basket served to elevate the transducers in the event of a water leak; to center the transducers within the vessel and consequently the source annulus; and finally, to space the transducers vertically to eliminate any shadow shielding effect between them. Paper towels were placed between the transducers to aid in separating them vertically. This basket is also in Figure 11 along with the vessel.

This basket also served these same functions for the Fricke dosimetry work found in Appendix A. The dose rate determined by the Fricke dosimetry was approximately 2000 rads/minute for the experimental period.

CHAPTER IV

EXPERIMENTAL DATA AND RESULTS

The data logs will be presented at the end of this chapter in order of increasing exposure received by the transducers beginning with log no. 5. Statements are included detailing the various specifics concerning some of the logs. The exposure for an irradiation period is taken from Figure 18 in Appendix A.

For logs no. 5 through 9 inclusive, the transducers were arranged in the basket from top to bottom--E, B, L, C. They filled the basket with the proper paper spacing. An Equitip Hardness Tester was available and was used to determine the Equitip hardness value (EHV) of the lucite wedges after each irradiation period. A high EHV "L" number indicates a hard wedge. This information was included for angle beam transducers. There was no evidence of water leakage into the irradiation vessel during the course of the experiment. For logs no. 5 through no. 9, the lucite wedges were assembled to the angle beam transducers prior to irradiation.

Log no. 4 in Table 2 is the pre-irradiation average of the transducer parameters. The wedge couplant on log no. 5 (Table 8) had begun to crack and dry out, as it would under normal operating conditions because of the time since preparation. The transducer

E wedge had a slight green-orange coloration but was still transparent. Its EHV value was 854. This was comparable to a control value of 856. The transducer B had a transparent faint yellow-green coloration. Its EHV value of 862 compared favorably with the control EHV of 865. Two sets of data were acquired for this log, and it was determined they were well within tolerance. Therefore, only one set of data was taken for the transducers on future logs.

The wedge coloration for log no. 7 (Table 10), after 20.73 Mrads, was the same as it appeared in log no. 5. The E wedge began to show some cracking in the left side screw thread. This resulted in uneven couplant thickness causing gain variations. New couplant was applied to both transducer/wedge assemblies. Tranducers E and B read EHV values of 846 and 854 respectfully.

The wedge coloration began to darken on log no. 8 (Table 11), after 25.26 Mrads. The wedges were still transparent and had EHV values of 834 and 856 for E and B respectfully. Both wedges had severe inter-wedge cracking and mounting screw hole thread cracking. In attempting to mount and dismount the transducers to their prospective wedges, further cracking, uneven couplant thickness, and possibly wedge warpage caused unusual gain readings. A general comparison was made with transducers B and E with no wedges to similar control transducers to isolate wedge problems from transducer problems. It was decided that the wedges would continue to be used for evaluation purposes.

In log no. 9 (Table 12), after 34.61 Mrads, the wedges had darkened in color and begun to break apart. The EHV was virtually

unattainable due to lack of inter-wedge support. These wedges were taken out of service at this point and control wedges were used for the remaining evaluations. A comparison of the control wedges versus the irradiated wedges is shown in Figure 12. Transducer C and L both had begun to bulge and crack on their contact faces. This is shown in Figure 13 and Figure 14.

Log no. 10 (Table 13), after 48.39 Mrads, documents that transducer C had a multi-faceted crack and bulging of the wear plate and could no longer be evaluated. Its terminal dose was found to be between 34.61 and 48.39 Mrads. Transducer E suffered the same fate at the same dose as shown in Figure 15. The wear plate on transducer L had also begun to bulge and crack.

The irradiation arrangement in the basket for the two remaining transducers was B on the bottom and L on the top.

Log no. 11 (Table 14), after 64.55 Mrads, revealed the increase in bulging and cracking of transducer L. The transducer was exposed once more simply out of curiosity. It was believed that the transducer should really have been condemned prior to this point. The wear plate condition could easily have accounted for the additional gain needs. Slight bulging was apparent on transducer B but did not appear to affect its performance.

Log no. 12 (Table 15), after 76.25 Mrads, revealed no real additional cracking of transducer L. Therefore, its terminal dose was between 48.39 Mrads and 64.55 Mrads. Transducer B was bulging considerably at this point but had not cracked. It was reinserted into the pit in approximately its normal location.

Figure 12

Comparison of Control Versus Irradiated Wedges

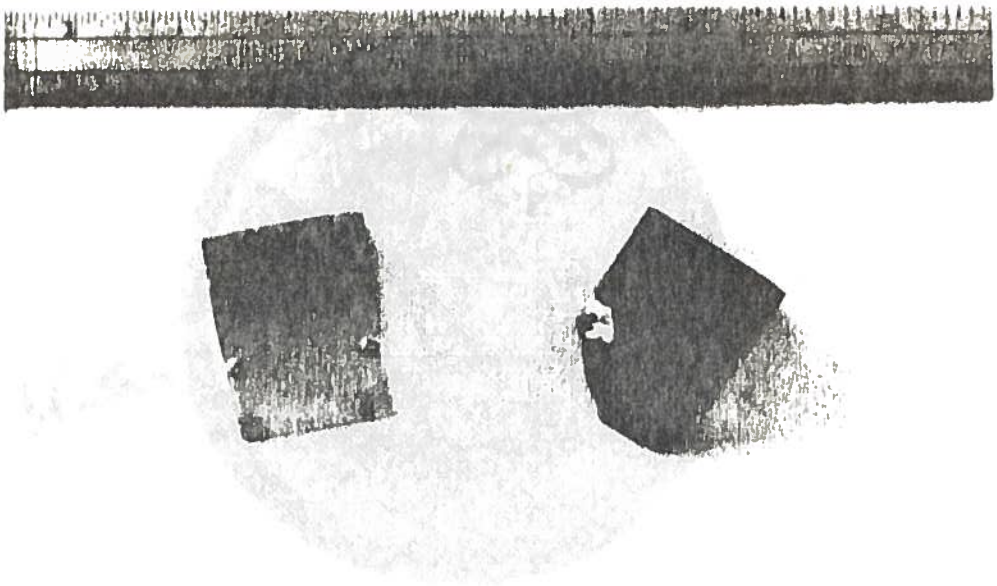

Type E Wedges

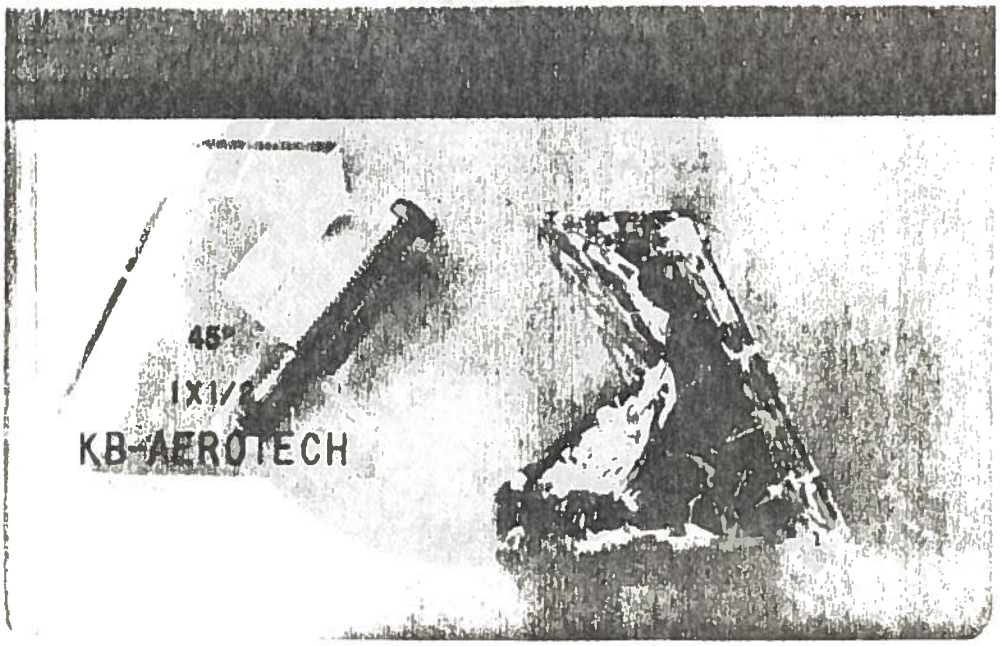

Type B Wedges

Figure 13

Transducer Wear Plate Cracking

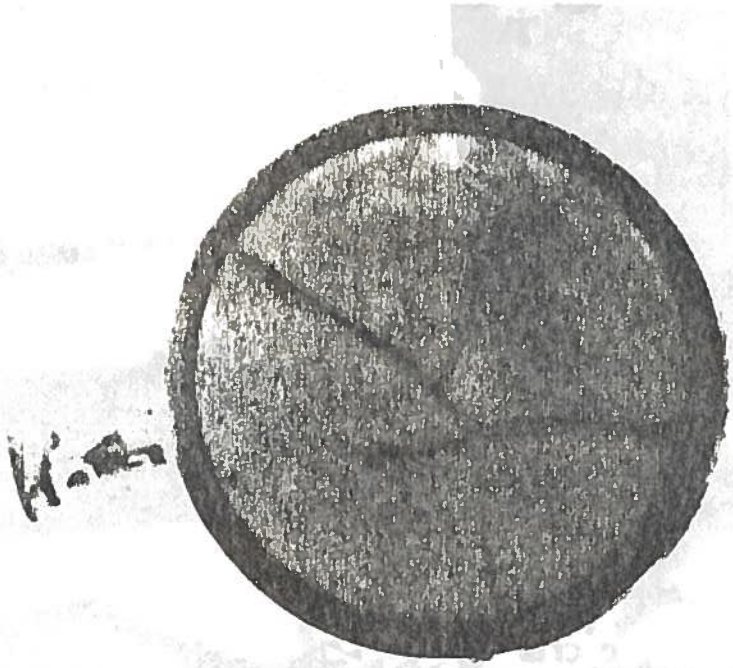

Type L

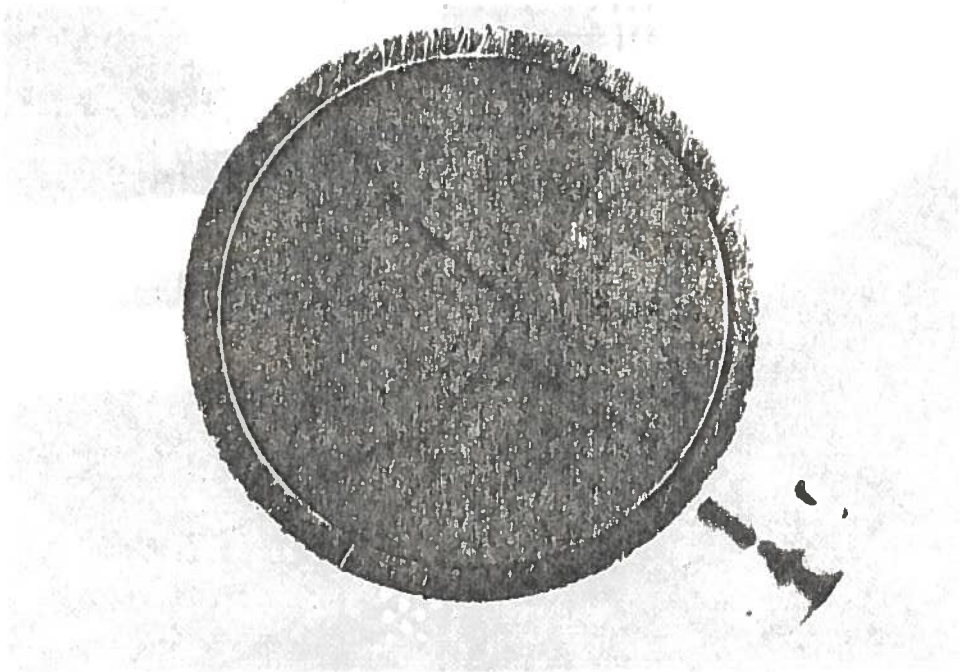

Type C

Figure 14

Normal Beam Transducer Bulging

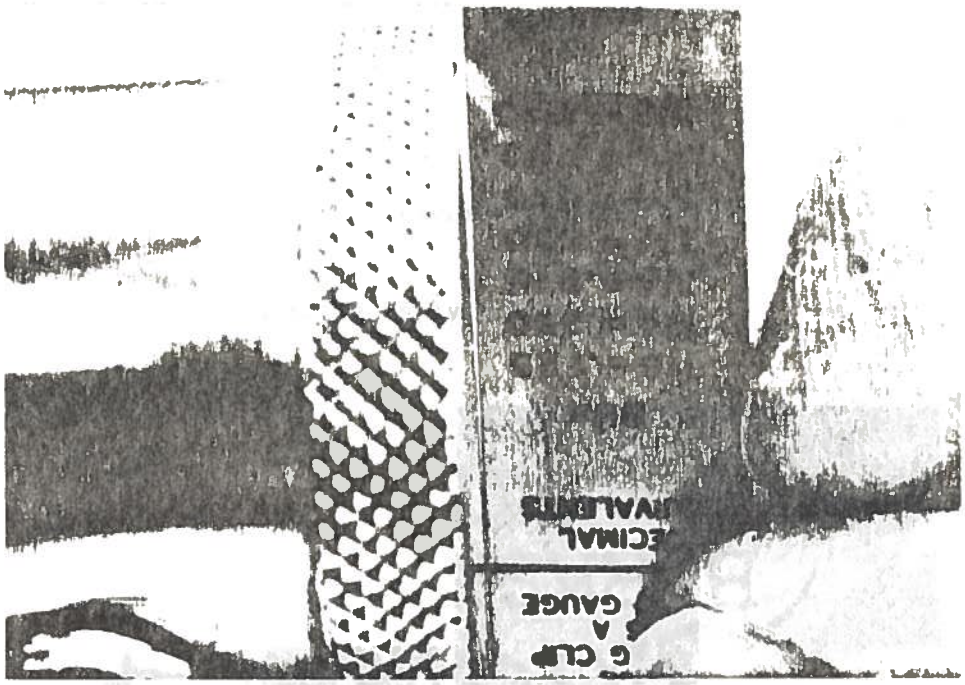

Type L

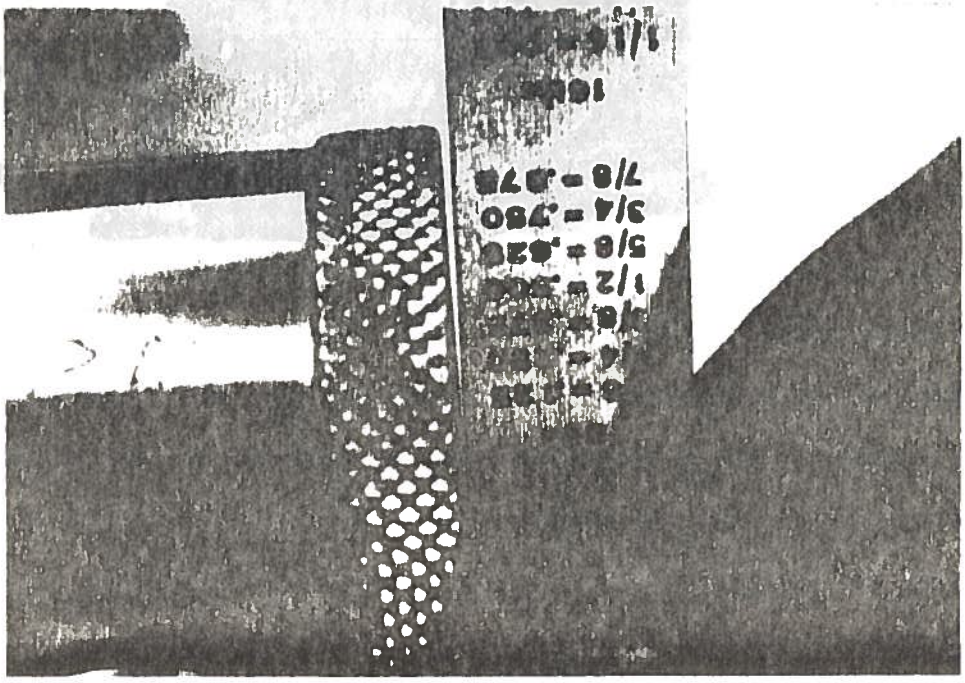

Type C

Figure 15

Bulging on Type E Transducer

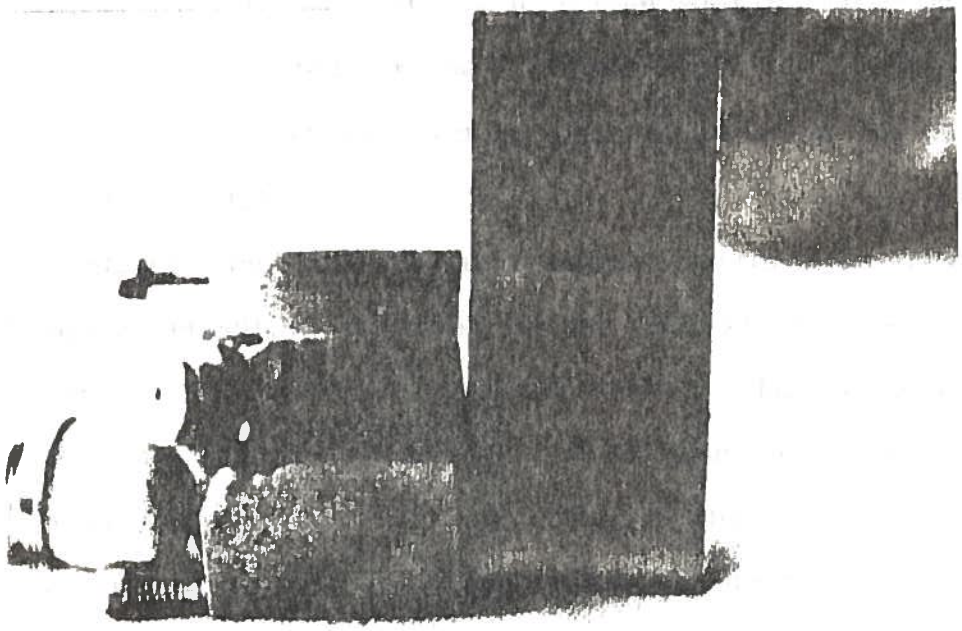

Log no. 15 (Table 18), after 115.98 Mrads, revealed extreme bulging of transducer B, as shown in Figure 16. A genuine doubt existed regarding the transducer's ability to even perform at all in a remote environment due to the bulging. It did appear, however, that the couplant was still able to diffuse fairly evenly in the transducer wedge interface.

The instrument cross-calibration was performed prior to the transducer B evaluation on log no. 17 (Table 20). A new control transducer was used and revealed a difference of +5 dB in signal amplitude, and a difference of -1% in screen width. The readings in Table 20 are corrected for these differences. The Branson 303 had a tolerance of 5% on the vertical amplitude whereas the USL-38 had a tolerance of 1.0%.

Throughout the course of the experiment, setting the artificial-defect signal reflections displayed on the CRT at the desired 90% screen height line was a difficult task. For example, a particular gain setting of 50 dB, would place the peak of a signal at 87% screen amplitude. Adjusting in the minimum increase in gain, 1 dB to 51 dB, would then place the signal peak at near 96% screen amplitude. Obviously one or the other gain setting had to be chosen and recorded along with percent screen amplitude. This complicated the task of assessing the transducers' performances. The method used to unravel the data is based on the dynamic range curve of the instrument (USL-38), Figure 17 and is a plot of the amplitude (%) versus gain (dB). The maximum variation in percent amplitude was determined for each transducer in each sensitivity evaluation. The crack reflection category of transducer B will be

Figure 16

Bulging on Type B Transducer

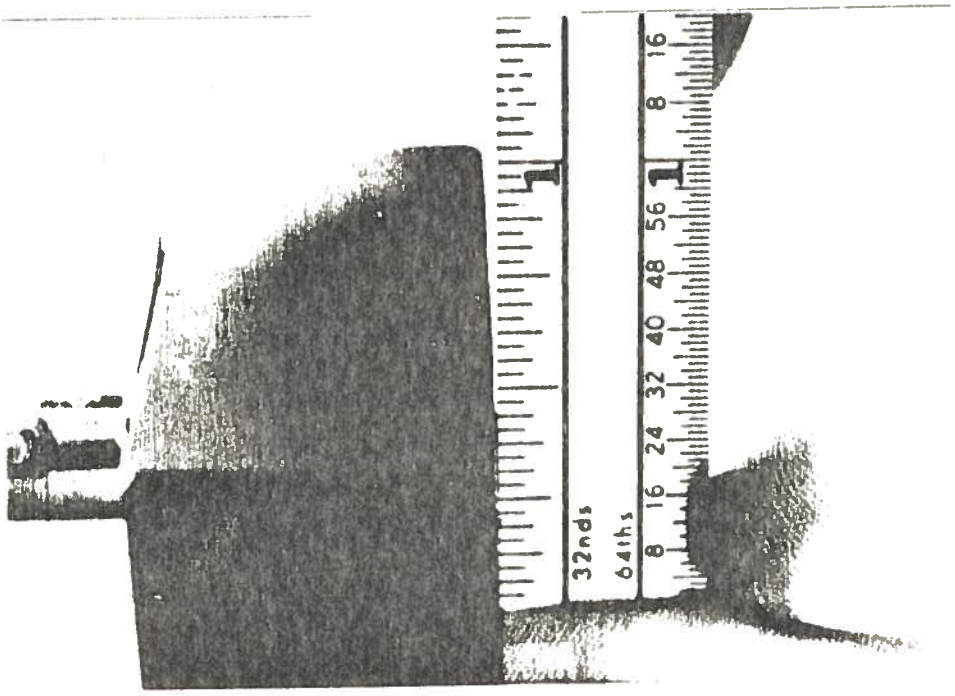

Figure 17

Dynamic Range Curve

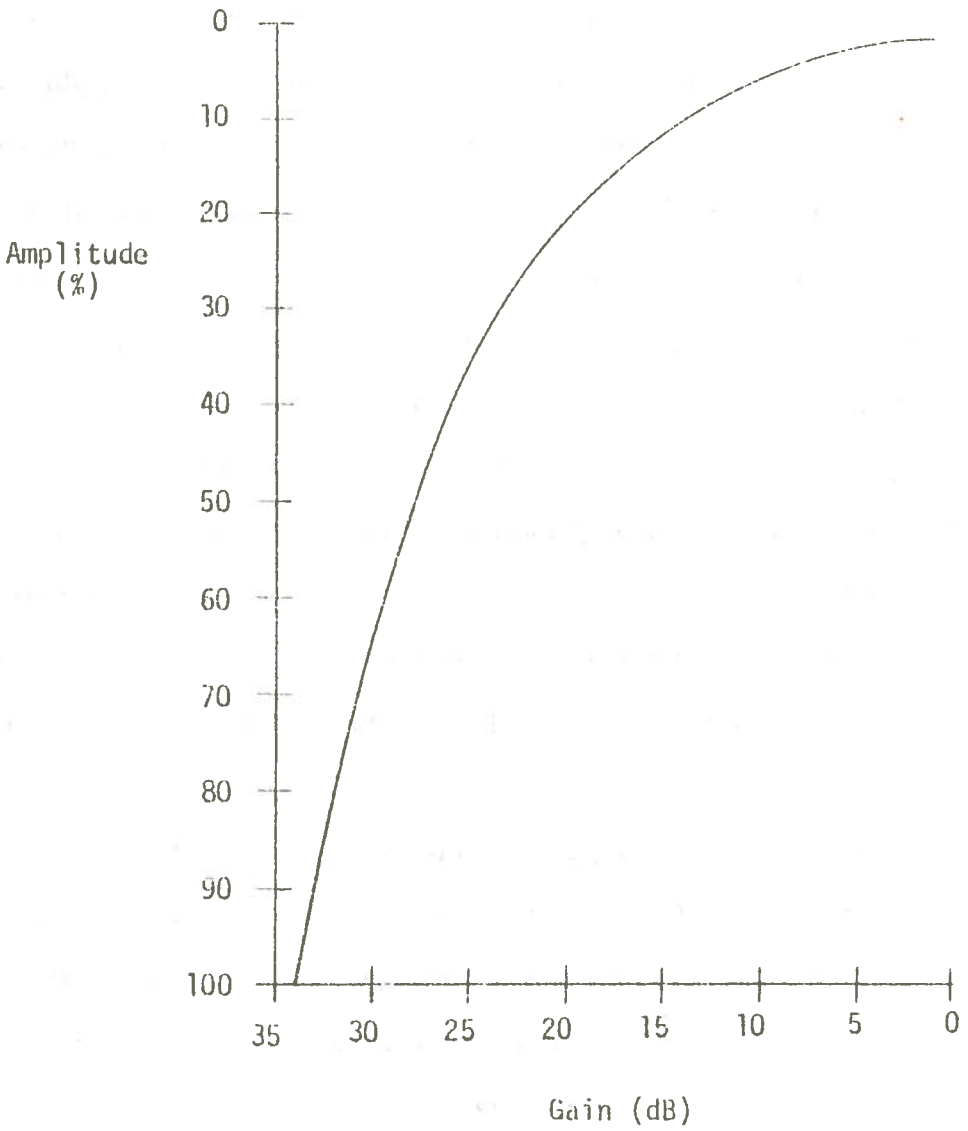

illustrated as follows. The reflected signal varied from 90% to 99% of screen height for the entire series of tests. This correlates to an amplitude variance of 9%. From Figure 17 it can be seen that this correlates to a minimum gain variance of ±1 dB. This then, would have to be added to the log tolerance of ±1 dB to yield a total maximum deviation of ±2 dB.

Experimental results tabulated in Table 4 through Table 7 were based on the following considerations. Using log no. 4 as a basis or normal, all initial evaluation values were assigned a standard value of zero (0). The gain in a particular category from each log fell into one of the following three categories. If the gain value was the same, the value was designated as having 0 variance, if the value was higher it was designated as having positive (+) variance, and if the value was lower it was designated as having negative (-) variance. This method only applied to the sensitivity data, but not to the "percent width" data, commonly referred to as resolution. The pre-irradiation evaluation log was also used as a basis for the resolution data. The values tabulated are the difference between the corresponding value in the log of question and the basis resolution value.

Although transducers L and C began trends toward loss of sensitivity between 34.61 Mrads and 48.39 Mrads, transducer E proved that sensitivity variations could easily be found when a different face of the multi-faceted wear plate was in contact with the wedge and consequently the test block. This phenomenon would allow different amounts of sound energy to be incident on the

TABLE 4

Resolution Data For The 0.062" Diameter Hole

Dose (Mrads)	Transducer Type L	C	B	E
0.00	0	0	0	0
6.14	0	+2	-1	-1
12.28	-1	0	-1	-1
20.73	0	+1	0	0
25.26	0	0	0	0
34.61	-1	0	+1	-1
48.39	0		+1	
64.55	0		+1	
76.25			+1	
90.11			+1	
98.99			+1	
115.98			+1	
138.13			+1	
186.53			+2	

TABLE 5

Data For The Second Plexiglass Reflection

Dose (Mrads)	Sensitivity L	Sensitivity C	Resolution L	Resolution C
0.00	0	0	0	0
6.14	-1	-2	0	0
12.28	-1	-2	0	0
20.73	-3	0	0	0
25.26	-1	+2	+1	+1
34.61	+1	+25	+1	
48.39	+2		-1	
64.55	+15		+1	
Variance	±1 dB	±1 dB		

TABLE 6

Data For The 3.6" Reflection

Dose (Mrads)	Sensitivity L	Sensitivity C	Resolution L	Resolution C
0.00	0	0	0	0
6.14	+2	+2	0	+1
12.28	+2	0	0	+1
20.73	+2	+2	+1	+1
25.26	+3	+4	+1	+1
34.61	+11	+15	+1	+1
48.39	+25		0	
64.55	+33		+1	
Variance	N/A	N/A		

TABLE 7

Data For The Crack Reflection

Dose (Mrads)	Sensitivity B	Sensitivity E	Resolution B	Resolution E
0.00	0	0	0	0
6.14	-2	+1	0	0
12.28	-2	+1	0	0
20.73	+2	+2	0	0
25.26	0	+13	0	0
34.61	0	+1	+1	0
48.39	0		0	
64.55	+1		0	
76.25	-1		0	
90.11	+1		0	
98.99	0		0	
115.98	-3		0	
138.13	0		0	
186.53	+21		0	
Variance	±1 dB	±1 dB		

artificial defect accounting for some of these variations. The resolution of the transducers was not significantly changed in any way. The evaluation point necessary to determine detectability was never attained as the 0.062" diameter hole was detectable throughout.

TABLE 8

Transducer Data Log Number 5

DATE: 6/28/82 IRRADIATED FROM: 11:05 A.M. 6/26/82 TO: 2:13 P.M. 6/28/82

TRANSDUCERS EXPOSED: 3068 Minutes TOTAL EXPOSURE TO DATE: 6.14 Mrads

Trans. type	Wedge exit point	Trans. angle Loc./ angle	Full screen (in.)	0.062" Hole Loc./ %width	0.062" Hole dB/ %amp.	Second Plex. Reflection Loc./ %width	Second Plex. Reflection dB/ %amp.	3.6" Reflection Maximum dB at baseline dB / %width	Crack Reflection Loc./ %width	Crack Reflection dB/ %amp.
L			2.0	29/11.	47/97					
			5.0			78/4.	57/89	35/4.		
C			2.0	30/10.	44/96					
			5.0			78/4.	64/95	40/5.		
B	As marked	60/45°	5.0	18/2.	68/91				42/2.	46/95
E	1 div. under std.	60/45°	5.0	16/2.	70/95				40/2.	38/86

TABLE 9

Transducer Data Log Number 6

DATE: 6/28/82 IRRADIATED FROM: 11:05 A.M. 6/26/82 TO: 2:13 P.M. 6/28/82

TRANSDUCERS EXPOSED: 3068 Minutes TOTAL EXPOSURE TO DATE: 12.28 Mrads

Trans. type	Wedge exit point	Trans. angle Loc./ angle	Full screen (in.)	0.062" Hole Loc./ %width	0.062" Hole dB/ %amp.	Second Plex. Reflection Loc./ %width	Second Plex. Reflection dB/ %amp.	3.6" Reflection Maximum dB at baseline dB / %width	Crack Reflection Loc./ %width	Crack Reflection dB/ %amp.
L			2.0	29/10.	46/85					
			5.0			78/4.	57/88	35/4.		
C			2.0	29/8.	45/95					
			5.0			78/4.	64/97	38/5.		
B	As marked	60/45°	5.0	18/2.	67/90				42/2.	46/97
E	1 div. under std.	60/45°	5.0	16/2.	68/82				40/2.	38/95

TABLE 10

Transducer Data Log Number 7

DATE: 7/1/82 IRRADIATED FROM: 8:17 P.M. 6/28/82 TO: 7:12 P.M. 7/1/82

TRANSDUCERS EXPOSED: 4255 Minutes TOTAL EXPOSURE TO DATE: 20.73 Mrads

Trans. type	Wedge exit point	Trans. angle Loc./ angle	Full screen (in.)	0.062" Hole Loc./ %width	0.062" Hole dB/ %amp.	Second Plex. Reflection Loc./ %width	Second Plex. Reflection dB/ %amp.	3.6" Reflection Maximum dB at baseline dB / %width	Crack Reflection Loc./ %width	Crack Reflection dB/ %amp.
L			2.0	29/11	43/93					
			5.0			79/4.	55/95	35/5.		
C			2.0	29/9.	46/91					
			5.0			79/4.	66/90	40/5.		
B	As marked	60/45°	5.0	17/3.	68/91				42/2.	50/93
E	1 div. over std.	60/45°	5.0	17/3.	72/95				41/2.	39/92

TABLE 11

Transducer Data Log Number 8

DATE: 7/3/82 IRRADIATED FROM: 9:23 P.M. 7/1/82 TO: 11:12 A.M. 7/3/82

TRANSDUCERS EXPOSED: 2267 Minutes TOTAL EXPOSURE TO DATE: 25.26 Mrads

Trans. type	Wedge exit point	Trans. angle Loc./ angle	Full screen (in.)	0.062" Hole Loc./ %width	0.062" Hole dB/ %amp.	Second Plex. Reflection Loc./ %width	Second Plex. Reflection dB/ %amp.	3.6" Reflection Maximum dB at baseline dB / %width	Crack Reflection Loc./ %width	Crack Reflection dB/ %amp.
L			2.0	30/11	46/92					
			5.0			79/5.	57/96	36/5.		
C			2.0	29/8.	47/91					
			5.0			78/4.	68/92	42/5.		
B	As marked	59/45°	5.0	18/3.	68/90				42/2.	48/97
E	1 div. under std.	61/45°	5.0	16/3.	78/93				40/2.	50/95

TABLE 12

Transducer Data Log Number 9

DATE: 7/6/82 IRRADIATED FROM: 1:10 P.M. 7/3/82 TO: 7:06 P.M. 7/6/82

TRANSDUCERS EXPOSED: 4676 Minutes TOTAL EXPOSURE TO DATE: 34.61 Mrads

Trans. type	Wedge exit point	Trans. angle Loc./ angle	Full screen (in.)	0.062" Hole Loc./ %width	0.062" Hole dB/ %amp.	Second Plex. Reflection Loc./ %width	Second Plex. Reflection dB/ %amp.	3.6" Reflection Maximum dB at baseline dB / %width	Crack Reflection Loc./ %width	Crack Reflection dB/ %amp.
L			2.0	29/10	50/95					
			5.0			79/5.	59/92	44/5.		
C			2.0	30/8.	52/98					
			5.0			79/5.	84/94	53/5.		
B	As marked	60/45°	5.0	18/4.	68/93				41/3.	48/94
E	As marked	60/45°	5.0	16/2.	71/98				42/2.	38/96

TABLE 13

Transducer Data Log Number 10

DATE: 7/11/82 IRRADIATED FROM: 8:56 P.M. 7/6/82 TO: 4:23 P.M. 7/11/82

TRANSDUCERS EXPOSED: 6927 Minutes TOTAL EXPOSURE TO DATE: 48.39 Mrads

Trans. type	Wedge exit point	Trans. angle Loc./ angle	Full screen (in.)	0.062" Hole Loc./ %width	0.062" Hole dB/ %amp.	Second Plex. Reflection Loc./ %width	Second Plex. Reflection dB/ %amp.	3.6" Reflection Maximum dB at baseline dB / %width	Crack Reflection Loc./ %width	Crack Reflection dB/ %amp.
L			2.0	30/11.	53/95					
			5.0			79/3.	60/95	58/4.		
B	As marked	60/45°	5.0	18/4.	68/96				42/2.	48/93

TABLE 14

Transducer Data Log Number 11

DATE: 7/18/82 IRRADIATED FROM: 7:32 P.M. 7/12/82 TO: 10:15 A.M. 7/18/82

TRANSDUCERS EXPOSED: 8143 Minutes TOTAL EXPOSURE TO DATE: 64.55 Mrads

Trans. type	Wedge exit point	Trans. angle Loc./ angle	Full screen (in.)	0.062" Hole Loc./ %width	0.062" Hole dB/ %amp.	Second Plex. Reflection Loc./ %width	Second Plex. Reflection dB/ %amp.	3.6" Reflection Maximum dB at baseline dB / %width	Crack Reflection Loc./ %width	Crack Reflection dB/ %amp.
L			2.0	30/11.	59/93					
			5.0			78/5.	73/96	66/5.		
B	As marked	60/45°	5.0	18/4.	67/95				42/2.	49/94

TABLE 15

Transducer Data Log Number 12

DATE: 7/22/82 IRRADIATED FROM: 11:12 A.M. 7/18/82 TO: 2:17 P.M. 7/22/82

TRANSDUCERS EXPOSED: 5945 Minutes TOTAL EXPOSURE TO DATE: 76.25 Mrads

Trans. type	Wedge exit point	Trans. angle Loc./ angle	Full screen (in.)	0.062" Hole Loc./ %width	0.062" Hole dB/ %amp.	Second Plex. Reflection Loc./ %width	Second Plex. Reflection dB/ %amp.	3.6" Reflection Maximum dB at baseline dB / %width	Crack Reflection Loc./ %width	Crack Reflection dB/ %amp.
B	As marked	60/45°	5.0	16/4.	69/98				40/2.	47/95

TABLE 16

Transducer Data Log Number 13

DATE: 7/27/82 IRRADIATED FROM: 3:07 P.M. 7/22/82 TO: 11:54 A.M. 7/27/82

TRANSDUCERS EXPOSED: 7007 Minutes TOTAL EXPOSURE TO DATE: 90.11 Mrads

Trans. type	Wedge exit point	Trans. angle Loc./ angle	Full screen (in.)	0.062" Hole Loc./ %width	0.062" Hole dB/ %amp.	Second Plex. Reflection Loc./ %width	Second Plex. Reflection dB/ %amp.	3.6" Reflection Maximum dB at baseline dB / %width	Crack Reflection Loc./ %width	Crack Reflection dB/ %amp.
B	As marked	60/45°	5.0	16/4.	68/92				42/2.	49/99

TABLE 17

Transducer Data Log Number 14

DATE: 8/2/82 IRRADIATED FROM: 12:24 P.M. 7/27/82 TO: 3:00 P.M. 7/30/82

TRANSDUCERS EXPOSED: 4476 Minutes TOTAL EXPOSURE TO DATE: 98.94 Mrads

Trans. type	Wedge exit point	Trans. angle Loc./ angle	Full screen (in.)	0.062" Hole Loc./ %width	0.062" Hole dB/ %amp.	Second Plex. Reflection Loc./ %width	Second Plex. Reflection dB/ %amp.	3.6" Reflection Maximum dB at baseline dB / %width	Crack Reflection Loc./ %width	Crack Reflection dB/ %amp.
B	As marked	60/45°	5.0	18/4.	67/97				43/2.	48/92

TABLE 1S

Transducer Data Log Number 15

DATE: 8/8/82 IRRADIATED FROM: 1:23 P.M. 8/2/82 TO: 1:32 P.M. 8/8/82

TRANSDUCERS EXPOSED: 8649 Minutes TOTAL EXPOSURE TO DATE: 115.98 Mrads

Trans. type	Wedge exit point	Trans. angle Loc./ angle	Full screen (in.)	0.062" Hole Loc./ %width	0.062" Hole dB/ %amp.	Second Reflection Loc./ %width	Second Plex. dB/ %amp.	3.6" Reflection Maximum dB at baseline dB / %width	Crack Reflection Loc./ %width	Crack Reflection dB/ %amp.
B	As marked	59 / 45°	5.0	16 / 4.	67 / 94				42 / 2.	45 / 96

TABLE 19

Transducer Data Log Number 16

DATE: 8/16/82 IRRADIATED FROM: 2:18 P.M. 8/8/82 TO: 10:37 A.M. 8/16/82

TRANSDUCERS EXPOSED: 11,262 Minutes TOTAL EXPOSURE TO DATE: 138.13 Mrads

Trans. type	Wedge exit point	Trans. angle Loc./ angle	Full screen (in.)	0.062" Hole Loc./ %width	0.062" Hole dB/ %amp.	Second Plex. Reflection Loc./ %width	Second Plex. Reflection dB/ %amp.	3.6" Reflection Maximum dB at baseline dB / %width	Crack Reflection Loc./ %width	Crack Reflection dB/ %amp.
B	As marked	60/45°	5.0	16/4.	68/97				42/2.	48/99

TABLE 20

Transducer Data Log Number 17

DATE: 9/2/82 IRRADIATED FROM: 11:20 A.M. 8/16/82 TO: 3:42 P.M. 9/2/82

TRANSDUCERS EXPOSED: 24,692 Minutes TOTAL EXPOSURE TO DATE: 186.53 Mrads

Trans. type	Wedge exit point	Trans. angle Loc./ angle	Full screen (in.)	0.062" Hole Loc./ %width	0.062" Hole dB/ %amp.	Second Plex. Reflection Loc./ %width	Second Plex. Reflection dB/ %amp.	3.6" Reflection Maximum dB at baseline dB / %width	Crack Reflection Loc./ %width	Crack Reflection dB/ %amp.
B	As marked	60/45°	5.0	18/2.	87/85				41/2.	69/90
B Corrected	As marked	60/45°	5.0	18/3.	82/85				41/3.	64/90

CHAPTER V

DISCUSSION, CONCLUSIONS, AND RECOMMENDATIONS

The two primary observations of the radiation effects on ultrasonic transducers exposed to large doses of gamma radiation are:

1. The wear plate bulged and cracked,
2. The lucite wedges discolored, cracked, and became brittle to a point of uselessness

The failure dose for the wedges was between approximately 25 and 35 Mrads. There was a wide failure dose range for the transducers. Each type of transducer exhibited wear plate distortion and cracking at different doses. The first failures were for transducers C and E in the dose range of approximately 35 to 48 Mrads. Type E is an angle-beam transducer and would have required removal from service earlier because of wedge failure. Transducer type L, a contact-type transducer, failed between approximately 48 and 65 Mrads. The type B transducer, the second of the two angle-beam transducers, withstood the greatest dose. It failed between approximately 138 and 187 Mrads. However, this transducer would have required removal from service much earlier because of wedge failure.

An important difference between the type B transducer, which survived the greatest dose, and the other three types is that it has an aluminum case. For all of the transducers, the major reason for failure appeared to be swelling of the epoxy potting material. This forced the wear plate to distort, and prohibited effective contact with the surface. As a result of this coupling problem, it was difficult to evaluate the transducers. There was no apparent deterioration of the piezoelectric crystal even at the highest dose.

The transducer with the stainless steel casing, transducer E, was cut in half and polished. When viewed under a microscope, the transducer was found to have extensive gas bubble formation and cracking in the epoxy. The majority of the bubbles and cracks were nearest the inside surface of the casing. It was readily apparent that the expanding epoxy caused bulging in the direction of the least support which was the contact surface of the transducer. Because of the epoxy expansion, the backing material and the piezoelectric crystal were cracked. The burnt-orange discoloration of the epoxy closely resembled the discoloration of the lucite wedges.

The radiation effect on the epoxy potting compound may provide an avenue for explaining the differences in failure-dose ranges for the aluminum cased and steel cased transducers. Gamma radiation will act directly on the epoxy material throughout the epoxy volume. However, near the casing the epoxy will also be irradiated by electrons ejected from the metal by gamma interactions. The ejected electrons will be more abundant for steel than for aluminum because of their different atomic numbers. A detail

derivation of the dose from these electrons is found in Appendix B. The results of the calculations for aluminum and steel casings revealed that the steel casing will lead to approximately twice the total gamma and electron dose than for the aluminum casing. This theoretical result is in reasonable agreement with the experimental observations.

Conclusions

The following conclusions may be drawn from the experimental observations in Chapter IV and the preceding discussion:

1. Standard UT transducers will fail at high radiation doses

2. Failure resulted from bulging of the wear plate and cracking of the piezoelectric crystal. The cause of these results appears to be radiation-induced expansion of the epoxy potting behind the crystal

3. The three steel-cased transducers failed at lower doses than the aluminum-cased transducer because of secondary wall-electron effects on the potting compound

4. Angle-beam transducers with lucite wedges will fail at the lowest dose because of wedge degradation

5. Piezoelectric activity does not appear to degrade at doses lower than those required to induce wear-plate distortion

6. Because of the similarities in construction, AE transducers would be expected to experience similar modes of failure

Assuming the average HLW canister would produce a dose of approximately 25 Mrads per day at its surface, the service time for the standard UT transducer would fall between two to three days.

Therefore, the monitoring of HLW canisters is not feasible with unshielded standard UT transducers.

Recommendations

Application of UT or AE monitoring for HLW canisters will require specially designed transducers or protection of the standard trasducer from intense radiation fields. Several options for protecting the transducers and wedges are possible. These include the use of a collar around the neck of the canister to function as a radiation shield. Attaching the transducer to a stainless steel wave guide that is appropriately welded to the closure plug area would reduce the dose received by the transducer approximately as the square of the wave guide length. Alternative wedge materials such as brass or bronze should be considered, or the wedge may be omitted if the transducers are properly permanently attached. Certainly these options and others may possibly be used simultaneously.

Even though the transducer could be protected somewhat by the techniques just described, development of a radiation-resistant transducer is desirable. Because similar degradation occurred in standard transducers exposed to high temperatures, the components used in high temperature transducer construction should improve their service time when subjected to high radiation doses. High temperature transducers consist of:

1. A tightly molecular bonded two-part epoxy compound or alternatively, an inorganic adhesive material

2. Lithium niobate piezoelectric crystals are commonly used because of their ability to perform at elevated temperatures (1000°C)

3. Ceramic wear plates are employed because they will also function at high temperatures

4. The use of permanently potted and stainless steel sheathed coaxial cables as integral parts of these transducers

As documented earlier, a low atomic number material should be used for the casing provided it is theoretically compatible with the other transducer components. This evaluation procedure could then be used to determine the gamma radiation effects on such a radiation-resistant UT transducer.

REFERENCES

1. Lee Dembart, "U.S. Ready to Decide Best Disposal of Nuclear Waste", The Los Angeles Times, [Los Angeles, California], July 13, 1981, p. 1-A.

2. B.J. Eberhard and J.W. Elker Jr., "High Current Resistance Welding of Nuclear Waste Containers", Welding Journal, vol. 61, (June 1982), pp. 15-19.

3. "New Problems Arise For Nuclear Waste Storage", Chemical and Engineering News, vol. 56, (June 12, 1978), p. 28.

4. Eberhard, loc. cit.

5. Bernard L. Cohen, "High-level Radioactive Waste From Light-water Reactors", Reviews of Modern Physics, vol. 49, no. 1, (January 1977), pp. 1-20.

6. Don Jolly, Southwest Research Institute, San Antonio, Texas, private correspondence, June 3, 1982.

7. Juan Ferrer, Physical Acoustics Cooperation, Princeton, New Jersey, private conversation, June 4, 1982.

8. B. Conroy, General Electric Nuclear Energy Group, San Jose, California, private conversation, June 3, 1982.

9. Jolly, loc. cit.

10. Ferrer, loc. cit.

11. Doug Lutz and Tom Carodiskey, Krautkramer-Branson Inc., Allentown, Pennsylvania, private conversation, June 2, 1982.

12. INIS Atomindex, Subject Index, vol. 12, January-December 1981.

13. Josef Krautkramer and Herbert Krautkramer, Ultrasonic Testing of Materials, 2nd ed., Springer-Verlag Berlin Heildelberg New York, 1977, 667 pp.

14. Ibid.

REFERENCES (Continued)

15. Krautkramer, loc. cit.

16. Jean-Claude Lenain, "General Principles of Acoustic Emission", Dunegan/Endevco Technical Report DE 78-5, January, 1979, 4 pp.

17. Metals Handbook, "Nondestructive Inspection and Quality Control", 8th ed., vol. 11, American Society For Metals, Metals Park, Ohio, 1976, 446 pp.

18. Krautkramer-Branson, Inc., 250 Long Beach Blvd., Stratford, CN.

19. Ibid.

20. Augustine O. Allen, The Radiation Chemistry of Water and Aqueous Solutions, D. Van Nostrand Company, Inc., Princeton, New Jersey, 1961, 204 pp.

21. Ibid.

22. Dr. R. C. McIlhenny, Louisiana State University, Nuclear Science Center, Baton Rouge, Louisiana, private correspondence, January 21, 1983.

23. Dr. J. C. Courtney, editor, A Handbook of Radiation Shielding Data, sponsored by: Nuclear Science Center, Louisiana State University, Baton Rouge and Shielding and Dosimetry Division American Nuclear Society, July, 1976, pp. 7-13.

APPENDIX A

Dose Rate Calculation

One of the most widely accepted "chemical dosimeters" is the air-saturated solution of ferrous sulfate in 0.8N H_2SO_4 called the Fricke dosimeter.[20] This system allows the ferrous iron to oxidize to the ferric state in gamma radiation fields. Hardwick pointed out that the quantity of ferric iron formed could be determined by the direct reading of the optical absorbancy of the solution with an ultraviolet-visible spectrophotometer reading when the molar extinction coefficient is known.[21] The radiation absorbed dose, defined as the "rad", can be related to the absorbance (A)

$$D \text{ (rads)} = (3.033 \times 10^4) \times A \ ,$$

in which

A = the logarithim of the ratio of incident light intensity to the transmitted light intensity.

The temperature correction usually necessary in this relation was found to be unity. The dose rate D' is simply

$$D' \text{ (rads/time)} = \frac{D \text{ (rads)}}{\text{time of exposure}} \ .$$

The transducer basket was used for several dosimetry vial runs. Multiple spectrophotometer readings were taken on each vial. The readings were averaged on the basis of transition time into the "crown source" and vertical dose gradients between vials to yield the dose rate on the day dosimetry was done.

Using the attenuation equation

$$I_t = I_o e^{-\frac{0.693}{T_{\frac{1}{2}}}(t)},$$

in which

I_o = original intensity (rads),

I_t = intensity after time t (rads),

$T_{\frac{1}{2}}$ = Co-60 half life (5.272 years),

t = time after I_o was measured (years).

The dose rate curve in Figure 18 was constructed from this relationship. The dose rate for each log was taken from Figure 18 based on the date nearest the middle date within the time period of the log. This dose rate was then multiplied by the exposure time for a particular log to yield the additional dose the transducers received for that log.

The ± 0.01 Mrad tolerance resulted mainly from the multiple averaging schemes employed. A full order of magnitude (±0.001 Mrad) was lost to account for the averaging.

Figure 18

Dose Rate Curve

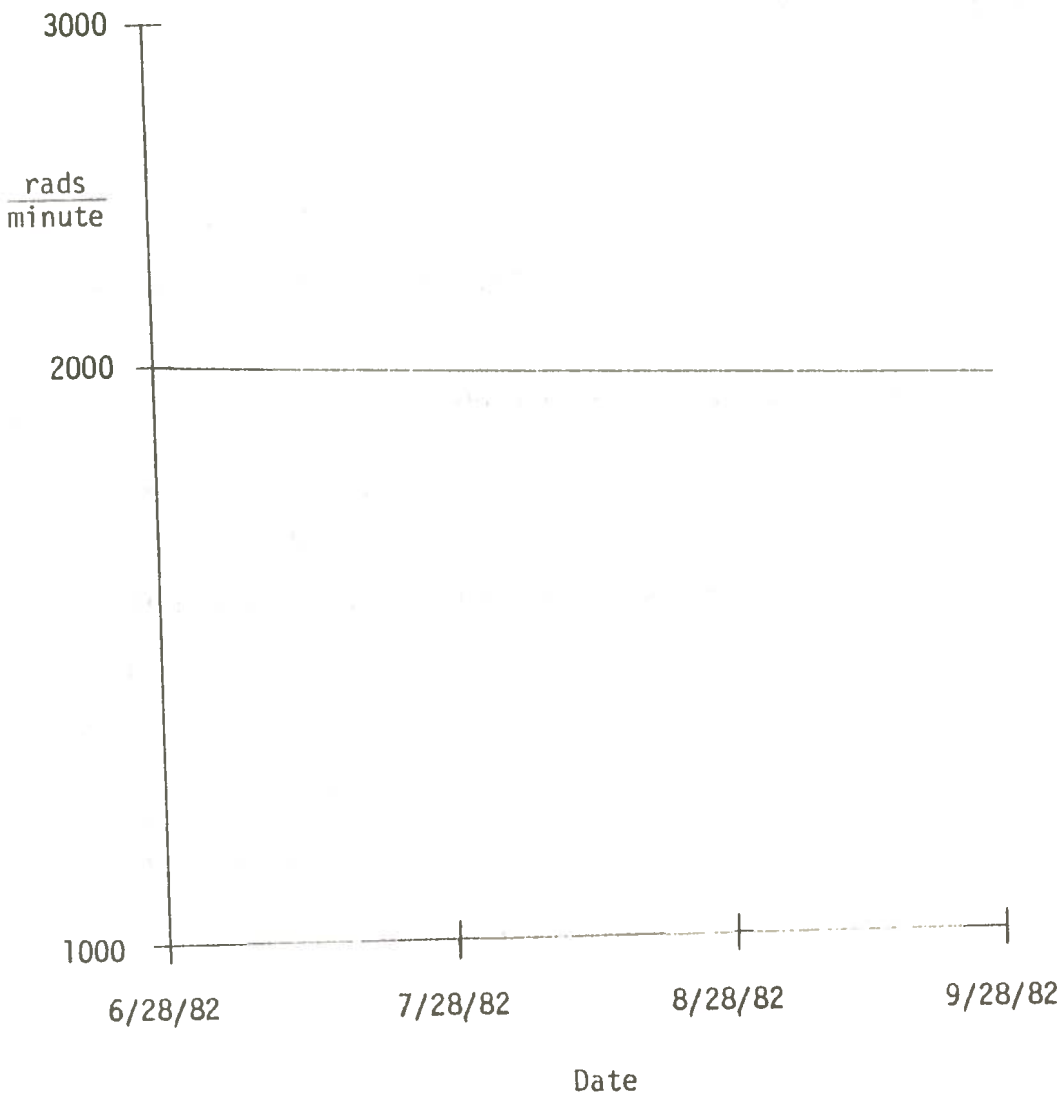

APPENDIX B

Epoxy Potting Dose Calculation[22]

Assume that 0.5 MeV is the energy deposited to the scattered electrons from the Co-60 gammas. Because of the limited range of the electrons, it will be assumed that the additional electron dose will occur near the casing only. The electron range (R_e) in a material is approximately

$$R_e = 500\ E_e\ (\text{MeV})\ \text{mg/cm}^2$$
$$= 250\ \text{mg/cm}^2.$$

The approximate density of the epoxy is

$$p_{\text{epoxy}} = 1\ \text{g/cm}^3.$$

Therefore, the linear range of the electron in the epoxy is

$$R_e = R_e/p_{\text{epoxy}} = 0.25/1.0$$
$$= 0.25\ \text{cm}.$$

From the attenuation equation for beta particles

$$I_{fx} = I_{fo}\ e^{-ux},$$

in which

I_{fo} = incident flux (no./cm^2-sec),

u = linear absorption coefficient (1/cm),

x = transducer casing thickness.

The change in flux becomes

$$I_{cf} = I_{fo} - I_{fx}$$
$$= I_{fo} (1 - e^{-ux}).$$

If ux is very much less than 1 then

$$e^{-ux} = 1-ux ,$$

so that

$$I_{cf} = I_{fo} [1 - (1 - ux)]$$
$$= uxI_{fo}.$$

If the electron flux is approximately equal to the change in gamma flux

$$I_{ef} = I_{cgf} ,$$

then

$$I_{ef} = (ux)_g I_{fog} ,$$

in which

$(ux)_g$ = aborption coefficient of the gammas,

I_{fog} = incident gamma flux,

within the casing. As an approximation of the electron flux at the inner transducer casing wall contributing to the epoxy dose

$$I_{ef} = 0.4 I_{cgf}$$
$$= 0.4 (uxI_{fo})_g .$$

Using the following conversion[23]

$$500 \text{ g/cm}^2\text{-sec} = 1 \text{ mrem/hr},$$

the number flux of electrons in aluminum becomes

$$N_{feA} = (ux)_g (500 \text{ g/cm}^2\text{-sec}),$$

in which

N_{feA} = number flux of electrons in aluminum,

$u = 0.0613 \text{ cm}^2/\text{gm}$ at 1.0 MeV,

$p = 2.699\ cm^3/gm,$

$x = 0.15$ cm on the average.

Therefore

$$N_{feA} = (0.0613)\ (2.699)\ (0.15)\ (500)$$
$$= 12.4\ e's/cm^2\text{-sec}.$$

Correcting this for the contributing electron current

$$N_{feAc} = (12.4)\ (0.4)$$
$$= 4.9\ e's/cm^2\text{-sec},$$

in the epoxy potting compound. Using the assumed electron energy, this becomes

$$E_{feAc} = 2.45\ MeV/cm^2\text{-sec},$$

with

E_{feAc} = energy flux of electrons contributing to the epoxy potting.

Assuming a maximum electron range of approximately 0.25 cm, the electron energy flux density for 500 g/cm^2-sec is

$$R_{ef} = 2.45/0.25 = 9.8\ MeV/cm^3\text{-sec}.$$

If

$$1\ MeV = 1.6 \times 10^{-6}\ ergs,$$

and

$$100\ ergs = 1\ rad = 1\ rem,$$

then

$$R_{ef} = (9.8)\ (1.6 \times 10^{-6})$$
$$= 1.57 \times 10^{-5}\ ergs/cm^3\text{-sec},$$

so that the dose from the electrons becomes

$$D_e = (1.57 \times 10^{-5})/100 = 1.57 \times 10^{-7}\ rads/sec$$
$$= 5.29 \times 10^{-4}\ rads/hr,$$

for 500 g/cm^2-sec. From the Fricke dosimetry work the maximum gamma dose is

$$D_g = (2000 \text{ rads/min}) (60 \text{ min/hr})$$
$$= 1.20 \times 10^5 \text{ rads/hr.}$$

Since there are 5.29×10^{-4} rads/hr of electrons for 1 Mrad/hr of gammas then the total electron dose to the epoxy becomes

$$D_e = (1.20 \times 10^5) (1000) (5.29 \times 10^{-4})$$
$$= 6.35 \times 10^4 \text{ rads/hr.}$$

Therefore the total epoxy potting dose from the aluminum transducer casing becomes

$$D_{tA} \text{ (rads/hr)} = D_g + D_e$$
$$= (1.20 \times 10^5) + (6.35 \times 10^4)$$
$$= 1.84 \times 10^5 \text{ rads/hr}$$
$$= 0.184 \text{ Mrads/hr.}$$

Because the mass attenuation coefficients are essentially identical for iron and aluminum at 1.0 MeV, and their densities are 7.87 g/cm^3 and 2.69 g/cm^3 respectfully, the dose calculation from the electrons will be approximately three times greater to the epoxy in the stainless steel cased transducer. Therefore, the total dose to the epoxy potting compound from the stainless steel transducer casing becomes

$$D_{tF} = (1.20 \times 10^5) + [3(6.35 \times 10^4)]$$
$$= 3.11 \times 10^5 \text{ rads/hr}$$
$$= 0.311 \text{ Mrads/hr.}$$

VITA

Robert W. Smilie was born in Baton Rouge, Louisiana, on October 31, 1955. He, with his family, lived in Southeast Asia for three years in the late 1960's, which concluded in a trip around the world. He returned to Baton Rouge and graduated from Central High School in 1973. He immediately entered Louisiana State University. In 1975 he entered Louisiana Tech University. In 1977 he returned to Louisiana State University, and obtained a Bachelor of Science degree in Industrial Technology in December of 1978.

He then began a professional career in Nondestructive Testing as an employee of Stroud Sales Company Incorporated. In August of 1982, he returned to Louisiana State University, to work toward completing a Master of Science degree in Nuclear Engineering. He had begun fulfilling the necessary requirements as a part time student in January of 1981. He is presently a candidate for a Master of Science in Nuclear Engineering.